

Metaplectic geometrical optics for modeling caustics in uniform and nonuniform media

N. A. Lopez¹ and I. Y. Dodin^{1,2}

¹*Department of Astrophysical Sciences, Princeton University, Princeton, New Jersey 08544, USA*

²*Princeton Plasma Physics Laboratory, Princeton, New Jersey 08543, USA*

As an approximate theory that is highly regarded for its computational efficiency, geometrical optics (GO) is widely used for modeling waves in various areas of physics. However, GO fails at caustics, which significantly limits its applicability. A new framework, called metaplectic geometrical optics (MGO), has recently been developed that allows caustics of certain types to be modeled accurately within the GO framework. Here, we extend MGO to the most general case. To illustrate our new theory, we also apply it to several sample problems, including calculations of two-dimensional wavefields near fold and cusp caustics. In contrast with traditional-GO solutions, the corresponding MGO solutions are finite everywhere and approximate well the true wavefield near these caustics.

I. INTRODUCTION

The propagation of waves in homogeneous and weakly inhomogeneous media is often described within the approximate theory known as geometrical optics (GO), or ray optics [1, 2]. However, GO fails at so-called caustics, where it predicts spurious singularities of the wavefield. Loosely speaking, caustics are surfaces across which the number of rays arriving at a given point changes abruptly [3]. The general properties of such surfaces have long been known from catastrophe theory, which provides a classification wherein only a finite number of caustic types are possible for a given number of spatial dimensions [4, 5]. This result underlies modern research into caustics [6–9], as general properties of a given caustic type can be inferred by studying a particular case. Still, practical calculations continue to rely on directly solving wave equations [10–12], which is computationally expensive. It would be advantageous to find a more efficient way to calculate these caustic structures. In particular, the question whether caustics can be modeled by somehow extending GO has been attracting attention for a long time.

One known solution to this problem is by Maslov [13], who proposed to rotate the ray phase space occasionally by $\pi/2$ using the Fourier transform (FT) in one or more spatial variables. Such rotations can remove caustics and locally reinstate GO, but they are inconvenient for simulations because the rotation points have to be introduced *ad hoc*, requiring the simulations to be supervised. In Refs. [14, 15], we proposed a modification of Maslov’s approach by replacing the FT with the metaplectic transform (MT), which might be familiar from other contexts such as aberration theory [16] and paraxial optics [17–19]. Using the MT, one can transform the wavefield continually along the rays, both eliminating the singularities at caustics and allowing for fully automated and fast simulations. This new framework, which we call metaplectic geometrical optics (MGO), has already been successfully benchmarked on one-dimensional (1-D) problems [15]. However, MGO as originally formulated in Refs. [14, 15] can still yield singularities in certain situations; thus, further progress is needed.

Here, we report a more general version of MGO, where the last spurious singularities are removed at the expense of additional calculations. We then demonstrate the reformulated MGO analytically on three examples: a homogeneous plane wave, a fold caustic, and a cusp caustic. In Arnold’s classification [20], they correspond to the A_1 , A_2 , and A_3 caustic types, respectively. The first case has no caustic *per se*; it is considered only to present a basic tutorial on the MGO machinery. The two other cases show how MGO leads to solutions that, unlike traditional-GO solutions, are finite everywhere and approximate well the true wavefield near the caustics.

This paper is organized as follows. In Sec. II, we review the basic equations of GO and MGO as described in Ref. [15]. In Sec. III, we report a more general version of MGO. In Sec. IV, we discuss three examples of the reformulated MGO, and we show analytically that MGO adequately approximates the wavefield in the entire space, even at caustics. In Sec. V, we summarize our main conclusions. Auxiliary calculations are presented in appendices and in the supplementary material.

II. OVERVIEW OF METAPLECTIC GEOMETRICAL OPTICS

We start by briefly reviewing the MGO method as it was presented in Ref. [15]. Let us consider a non-driven linear wave in a general linear medium. We do not assume any particular wave equation in this paper, as our theory is sufficiently general to handle any linear wave equation. That said, we shall restrict the analysis to scalar equations for simplicity. (Generalization to vector waves on non-Euclidean spaces is possible using the machinery presented in Ref. [21].)

Specifically, we assume that the wave is described by a scalar field ψ and governed by an integral equation

$$\int d\mathbf{q}' D(\mathbf{q}, \mathbf{q}') \psi(\mathbf{q}') = 0. \quad (1)$$

Here, \mathbf{q} is the coordinate on an N -D Euclidean (or pseudo-Euclidean) space, called \mathbf{q} -space, and $D(\mathbf{q}, \mathbf{q}')$ is the dispersion kernel. In particular, differential wave

equations (partial or ordinary) have dispersion kernels that consist of delta functions and their derivatives. For example, the Helmholtz equation has $D(\mathbf{q}, \mathbf{q}') = \nabla'^2 \delta(\mathbf{q}' - \mathbf{q}) + n^2(\mathbf{q}') \delta(\mathbf{q}' - \mathbf{q})$, where ∇' is the gradient with respect to \mathbf{q}' and $n(\mathbf{q})$ is a spatially varying index of refraction. (See Sec. IV for more examples.) More generally, the kernel D can be a smooth function, as is the case for waves in warm plasma, for example. (A review of the general theory of linear dispersion can be found in Ref. [22].) It is not necessary for our purposes to specify this function; let us simply state that D encodes all information about the linear medium where the wave propagates, whatever that medium may be.

Consider also \mathbf{p} -space, which is the Fourier-dual of \mathbf{q} -space. Then, \mathbf{q} -space and \mathbf{p} -space collectively define a $2N$ -D phase space with coordinates (\mathbf{q}, \mathbf{p}) . The dispersion kernel $D(\mathbf{q}, \mathbf{q}')$ can be associated with a function on phase space via the transformation

$$\mathcal{D}(\mathbf{q}, \mathbf{p}) \doteq \int d\mathbf{s} e^{i\mathbf{p}^\top \mathbf{s}} D\left(\mathbf{q} - \frac{\mathbf{s}}{2}, \mathbf{q} + \frac{\mathbf{s}}{2}\right), \quad (2)$$

where the integral is taken over \mathbf{q} -space and \doteq denotes definitions. (Note that vectors are interpreted as row vectors unless explicitly transposed via $^\top$, so $\mathbf{p}^\top \mathbf{s} = \mathbf{p} \cdot \mathbf{s}$.) The function $\mathcal{D}(\mathbf{q}, \mathbf{p})$ is known as the Weyl symbol of $D(\mathbf{q}, \mathbf{q}')$. We shall now analyze Eq. (1) in the short-wavelength limit using both traditional GO and MGO. Specifically, we assume in the following that the medium parameters, the wave envelope, and the wavelength itself vary slowly over a characteristic wavelength [1, 2, 21].

A. Traditional geometrical optics

In traditional GO, $\psi(\mathbf{q})$ is assumed to take the eikonal form given by

$$\psi(\mathbf{q}) = \phi(\mathbf{q}) e^{i\theta(\mathbf{q})}, \quad (3)$$

where $\phi(\mathbf{q})$ is a slowly varying envelope and $\theta(\mathbf{q})$ is a rapidly varying phase. Then, to the lowest order, Eqs. (1)-(3) yield the local dispersion relation [2, 21]

$$\mathcal{D}[\mathbf{q}, \mathbf{k}(\mathbf{q})] = 0, \quad (4)$$

along with the envelope transport equation

$$\mathbf{v}(\mathbf{q})^\top \partial_{\mathbf{q}} \log \phi(\mathbf{q}) = -\frac{1}{2} \partial_{\mathbf{q}} \cdot \mathbf{v}(\mathbf{q}). \quad (5)$$

Here, the local wavevector $\mathbf{k}(\mathbf{q})$ and the local group velocity $\mathbf{v}(\mathbf{q})$ are defined as

$$\mathbf{k}(\mathbf{q}) \doteq \partial_{\mathbf{q}} \theta(\mathbf{q}), \quad \mathbf{v}(\mathbf{q}) \doteq \partial_{\mathbf{p}} \mathcal{D}(\mathbf{q}, \mathbf{p})|_{\mathbf{p}=\mathbf{k}(\mathbf{q})}. \quad (6)$$

Hence, $\mathbf{k}(\mathbf{q})$ is irrotational, meaning that

$$\partial_{q_\ell} k_m = \partial_{q_m} k_\ell, \quad \ell, m = 1, \dots, N. \quad (7)$$

Equations (4) and (5) are commonly solved along the characteristic rays that satisfy

$$\partial_{\tau_1} \mathbf{q}(\boldsymbol{\tau}) = \partial_{\mathbf{k}} \mathcal{D}[\mathbf{q}(\boldsymbol{\tau}), \mathbf{k}(\boldsymbol{\tau})], \quad (8a)$$

$$\partial_{\tau_1} \mathbf{k}(\boldsymbol{\tau}) = -\partial_{\mathbf{q}} \mathcal{D}[\mathbf{q}(\boldsymbol{\tau}), \mathbf{k}(\boldsymbol{\tau})]. \quad (8b)$$

For integrable systems, these rays trace out an N -D surface in phase space called the dispersion manifold. We then define $\boldsymbol{\tau} \doteq (\tau_1, \dots, \tau_N)$ as coordinates on the dispersion manifold, with τ_1 serving as the longitudinal coordinate along a ray. Initial conditions provide $\mathbf{q}(0, \boldsymbol{\tau}_\perp)$ and $\mathbf{k}(0, \boldsymbol{\tau}_\perp)$, where $\boldsymbol{\tau}_\perp \doteq (\tau_2, \dots, \tau_N)$. For example, τ_1 can be the time variable or one of the spatial coordinates; then $\boldsymbol{\tau}_\perp$ are the remaining spatial coordinates.

The wavevector $\mathbf{k}(\mathbf{q})$ is determined from the rays as

$$\mathbf{k}(\mathbf{q}) = \mathbf{k}[\boldsymbol{\tau}(\mathbf{q})], \quad (9)$$

where $\boldsymbol{\tau}(\mathbf{q})$ is the function inverse to $\mathbf{q}(\boldsymbol{\tau})$. Although Eqs. (8) show that rays cannot cross in phase space, their projections onto \mathbf{q} -space can. As a result, $\boldsymbol{\tau}(\mathbf{q})$ is generally multivalued, meaning $\mathbf{k}(\mathbf{q})$ is as well. The envelope is constructed along the rays as

$$\phi[\mathbf{q}(\boldsymbol{\tau})] = \phi[\mathbf{q}(0, \boldsymbol{\tau}_\perp)] \sqrt{\frac{j(0, \boldsymbol{\tau}_\perp)}{j(\boldsymbol{\tau})}}, \quad (10)$$

where $\phi[\mathbf{q}(0, \boldsymbol{\tau}_\perp)]$ is set by initial conditions, and

$$j(\boldsymbol{\tau}) \doteq \det \partial_{\boldsymbol{\tau}} \mathbf{q}(\boldsymbol{\tau}). \quad (11)$$

Then, the total wavefield is constructed as

$$\psi(\mathbf{q}) = \sum_{\mathbf{t} \in \boldsymbol{\tau}(\mathbf{q})} \phi[\mathbf{q}(\mathbf{t})] \exp\left[i \int d\mathbf{q}^\top \mathbf{k}(\mathbf{q})\right], \quad (12)$$

where the summation is taken over all branches of $\boldsymbol{\tau}(\mathbf{q})$.

Clearly, $\psi(\mathbf{q})$ diverges where $j(\mathbf{t}) = 0$. Such points are caustics, and by Eq. (11), they occur where the dispersion manifold has a singular projection onto \mathbf{q} -space. To extend GO modeling to caustics and the neighboring regions, Ref. [15] proposed MGO, which we now describe.

B. Metaplectic geometrical optics

MGO also uses the rays provided by Eqs. (8) to solve Eq. (4). However, in MGO, the phase space is not fixed but instead is continually rotated, $(\mathbf{q}, \mathbf{p}) \rightarrow (\mathbf{Q}_t, \mathbf{P}_t)$, such that the local projection of the dispersion manifold onto \mathbf{Q}_t -space is always well-behaved. Accordingly, the envelope equation (5) is replaced with a similar envelope equation in the rotated frame that has no caustics by construction. This is done as follows.

Let us assume that the dispersion manifold $(\mathbf{q}, \mathbf{p}) = (\mathbf{q}(\boldsymbol{\tau}), \mathbf{k}(\boldsymbol{\tau}))$ has been obtained by integrating Eqs. (8) and consider the tangent plane at $\boldsymbol{\tau} = \mathbf{t}$. We can rotate our original phase space to align \mathbf{q} -space with the

tangent plane at \mathbf{t} (\mathbf{Q}_t -space) using the following linear transformation:

$$\mathbf{Q}_t = \mathbf{A}_t \mathbf{q} + \mathbf{B}_t \mathbf{p}, \quad \mathbf{P}_t = \mathbf{C}_t \mathbf{q} + \mathbf{D}_t \mathbf{p}, \quad (13)$$

where \mathbf{P}_t is Fourier-dual to \mathbf{Q}_t and the matrices \mathbf{A}_t , \mathbf{B}_t , \mathbf{C}_t , and \mathbf{D}_t are all $N \times N$. In Eq. (13), we require that

$$\mathbf{S}_t \doteq \begin{pmatrix} \mathbf{A}_t & \mathbf{B}_t \\ \mathbf{C}_t & \mathbf{D}_t \end{pmatrix} \quad (14)$$

be symplectic, that is,

$$\mathbf{S}_t \mathbf{J} \mathbf{S}_t^\top = \mathbf{J}, \quad \mathbf{J} \doteq \begin{pmatrix} 0_N & \mathbf{I}_N \\ -\mathbf{I}_N & 0_N \end{pmatrix}, \quad (15)$$

where 0_N and \mathbf{I}_N are respectively the $N \times N$ null and identity matrices. (A practical algorithm for computing \mathbf{S}_t from the ray trajectories using Gram–Schmidt orthogonalization is provided in Ref. [15].)

The transformation of the wavefield corresponding to the symplectic transformation (14) of the ray phase space is the MT [14, 23], sometimes called the linear canonical transform. The MT is a linear integral transformation from ψ to a new function Ψ given explicitly as

$$\Psi(\mathbf{Q}) = \int d\mathbf{q} M(\mathbf{Q}, \mathbf{q}) \psi(\mathbf{q}), \quad (16)$$

where the MT kernel is given as

$$M(\mathbf{Q}, \mathbf{q}) \doteq \frac{\sigma \exp[iG(\mathbf{q}, \mathbf{Q})]}{(2\pi i)^{N/2} \sqrt{\det \mathbf{B}}}, \quad (17)$$

and $G(\mathbf{q}, \mathbf{Q})$ is the following quadratic phase function:

$$G(\mathbf{q}, \mathbf{Q}) \doteq \frac{1}{2} \mathbf{Q}^\top \mathbf{D} \mathbf{B}^{-1} \mathbf{Q} - \mathbf{Q}^\top \mathbf{B}^{-\top} \mathbf{q} + \frac{1}{2} \mathbf{q}^\top \mathbf{B}^{-1} \mathbf{A} \mathbf{q}. \quad (18)$$

(Here, $^{-\top}$ denotes the matrix inverse transpose.) Each \mathbf{S} actually has two corresponding MTs that differ by an overall sign, which is designated by $\sigma \doteq \pm 1$. Note that Eq. (17) requires $\det \mathbf{B} \neq 0$; this requirement will be lifted in Sec. III A. Also note that the MT reduces to the familiar FT when $\mathbf{S} = \mathbf{J}$.

Let $\Psi_t(\mathbf{Q}_t)$ be the MT of $\psi(\mathbf{q})$ corresponding to \mathbf{S}_t of Eq. (14) (for a chosen MT sign convention). In MGO, we assume that $\Psi_t(\mathbf{Q}_t)$ [not $\psi(\mathbf{q})$] has the eikonal form

$$\Psi_t(\mathbf{Q}_t) = \Phi_t(\mathbf{Q}_t) e^{i\Theta_t(\mathbf{Q}_t)}, \quad (19)$$

where Φ_t is a slowly varying complex envelope and Θ_t is a phase that varies rapidly with the new coordinate \mathbf{Q}_t ; hence, $\mathbf{K}_t(\mathbf{Q}_t) \doteq \partial_{\mathbf{Q}_t} \Theta_t(\mathbf{Q}_t)$ is understood as the local wavevector in \mathbf{Q}_t -space. The eikonal approximation (19) is facilitated by the fact that $\partial_{\tau_1} \mathbf{K}_t = -\partial_{\mathbf{Q}_t} \tilde{\mathcal{D}} = \mathbf{0}$ at the tangent point by definition, where

$$\tilde{\mathcal{D}}(\mathbf{Q}_t, \mathbf{P}_t) = \mathcal{D}(\mathbf{D}_t^\top \mathbf{Q}_t - \mathbf{B}_t^\top \mathbf{P}_t, -\mathbf{C}_t^\top \mathbf{Q}_t + \mathbf{A}_t^\top \mathbf{P}_t), \quad (20)$$

is the Weyl symbol of the dispersion operator in the new coordinates. (We also assume that $\partial_{\tau_1} \mathbf{K}_t$ is slowly varying in the neighborhood of the tangent point.)

As shown in Ref. [15], taking the MT of Eq. (1) and performing the standard GO procedure in \mathbf{Q}_t -space using Eq. (19) yields equations similar to Eqs. (4) and (5) in the new variables. Specifically, the local dispersion relation has the form

$$\tilde{\mathcal{D}}[\mathbf{Q}_t, \mathbf{K}_t(\mathbf{Q}_t)] = 0, \quad (21)$$

and the envelope transport equation becomes

$$\mathbf{V}_t(\mathbf{Q}_t)^\top \partial_{\mathbf{Q}_t} \log \Phi_t(\mathbf{Q}_t) = -\frac{1}{2} \partial_{\mathbf{Q}_t} \cdot \mathbf{V}_t(\mathbf{Q}_t). \quad (22)$$

Here, we have introduced

$$\mathbf{V}_t(\mathbf{Q}_t) \doteq \partial_{\mathbf{P}_t} \tilde{\mathcal{D}}(\mathbf{Q}_t, \mathbf{P}_t)|_{\mathbf{P}_t = \mathbf{K}_t(\mathbf{Q}_t)}, \quad (23)$$

which is the corresponding group velocity.

If Eq. (4) is satisfied along the original rays, then Eq. (21) is satisfied along the rotated rays given by

$$\mathbf{Q}_t(\tau) = \mathbf{A}_t \mathbf{q}(\tau) + \mathbf{B}_t \mathbf{k}(\tau), \quad (24a)$$

$$\mathbf{K}_t(\tau) = \mathbf{C}_t \mathbf{q}(\tau) + \mathbf{D}_t \mathbf{k}(\tau). \quad (24b)$$

Hence, the dispersion manifold simply rotates with the ambient phase space¹.

Before solving Eq. (22), it is convenient to renormalize $\Psi_t(\mathbf{Q}_t)$ by its value at $\mathbf{Q}_t(\mathbf{t})$; that is, let

$$\Psi_t(\mathbf{Q}_t) = \alpha_t \Phi_t(\mathbf{Q}_t) e^{i\Theta_t(\mathbf{Q}_t)}, \quad \alpha_t \doteq \Psi_t[\mathbf{Q}_t(\mathbf{t})], \quad (25)$$

and require

$$\Phi_t[\mathbf{Q}_t(\mathbf{t})] = 1, \quad \Theta_t[\mathbf{Q}_t(\mathbf{t})] = 0. \quad (26)$$

Then, analogous to Eq. (10), Eq. (22) is solved to yield

$$\Phi_t[\mathbf{Q}_t(\tau)] = \Phi_t[\mathbf{Q}_t(t_1, \tau_\perp)] \sqrt{\frac{J_t(t_1, \tau_\perp)}{J_t(\tau)}}, \quad (27)$$

where $\Phi_t[\mathbf{Q}_t(t_1, \tau_\perp)]$ is set by initial conditions subject to Eq. (26), and

$$J_t(\tau) \doteq \det \partial_\tau \mathbf{Q}_t(\tau). \quad (28)$$

The phase can also be immediately determined as

$$\Theta_t(\mathbf{Q}_t) = \int_{\mathbf{Q}_t(\mathbf{t})}^{\mathbf{Q}_t} d\mathbf{Q}^\top \mathbf{K}_t(\mathbf{Q}), \quad (29)$$

where the line integral is taken over any path with the specified endpoints, and $\mathbf{K}_t(\mathbf{Q}_t)$ is constructed as

$$\mathbf{K}_t(\mathbf{Q}_t) = \mathbf{K}_t[\tau(\mathbf{Q}_t)], \quad (30)$$

¹ This is analogous to Wigner functions being simply rotated by fractional FTs [24].

where $\tau(\mathbf{Q}_t)$ is the function inverse to $\mathbf{Q}_t(\tau)$. Note that $\mathbf{K}_t(\mathbf{Q}_t)$ will generally be multivalued, so it must be restricted to the branch satisfying $\mathbf{K}_t[\mathbf{Q}_t(\mathbf{t})] = \mathbf{K}_t(\mathbf{t})$.

By continuity, α_t evolves along the rays as

$$\alpha_t = \alpha_{(0,t_\perp)} \exp \left[\int_0^{t_1} dh \eta_{(h,t_\perp)} \right], \quad (31)$$

where $\alpha_{(0,t_\perp)}$ is determined by initial conditions and

$$\begin{aligned} \eta_t &\doteq \frac{i}{2} \mathbf{K}_t^\top(\mathbf{t}) \mathbf{W}_t \mathbf{K}_t(\mathbf{t}) - \frac{i}{2} \mathbf{Q}_t^\top(\mathbf{t}) \mathbf{U}_t \mathbf{Q}_t(\mathbf{t}) - \frac{1}{2} \text{tr}(\mathbf{V}_t) \\ &+ \left[\partial_h \mathbf{Q}_t(\mathbf{t}) - \mathbf{V}_t^\top \mathbf{Q}_t(\mathbf{t}) - \mathbf{W}_t^\top \mathbf{K}_t(\mathbf{t}) \right]^\top \\ &\times \left\{ \partial_{\mathbf{Q}} \Phi_t[\mathbf{Q}_t(\mathbf{t})] + i \mathbf{K}_t(\mathbf{t}) \right\}. \end{aligned} \quad (32)$$

Here, the $N \times N$ matrices \mathbf{U}_t , \mathbf{V}_t , and \mathbf{W}_t are defined via

$$(\partial_h \mathbf{S}_t) \mathbf{S}_t^{-1} \doteq \begin{pmatrix} \mathbf{V}_t^\top & \mathbf{W}_t \\ -\mathbf{U}_t & -\mathbf{V}_t \end{pmatrix}, \quad (33)$$

where the directional derivative, defined as $h \partial_h \doteq \mathbf{h}^\top \partial_t$, should be interpreted as a total derivative acting on arguments and subscripts containing \mathbf{t} . (An alternate algorithm for evolving α_t based on successive applications of a near-identity MT [14] is provided in Ref. [15].)

Applying an inverse MT then maps $\Psi_t(\mathbf{Q}_t)$ to a function on \mathbf{q} -space, denoted $\psi_t(\mathbf{q})$, as

$$\psi_t(\mathbf{q}) = \int d\mathbf{Q}_t M_t^{-1}(\mathbf{q}, \mathbf{Q}_t) \Psi_t(\mathbf{Q}_t), \quad (34)$$

where the inverse MT kernel is given as

$$M_t^{-1}(\mathbf{q}, \mathbf{Q}_t) \doteq \frac{\sigma_t \exp[-iG_t(\mathbf{q}, \mathbf{Q}_t)]}{(-2\pi i)^{N/2} \sqrt{\det \mathbf{B}_t}}. \quad (35)$$

The overall sign factor σ_t must change whenever $\det \mathbf{B}_t$ crosses the branch cut of the square root to maintain continuity. This change in σ_t is related to the discrete phase jumps a wavefield experiences upon traversing a caustic.

At this point, semiclassical methods like GO and Maslov's method traditionally evaluate Eq. (34) using the stationary-phase approximation (SPA) about the ray contribution $\mathbf{Q}_t = \mathbf{Q}_t(\mathbf{t})$ [25]. However, the SPA fails when saddlepoints are close together [26], as occurs near caustics. To remedy this, note that under fairly general conditions, integrals like Eq. (34) can be evaluated on the union of steepest-descent contours through some subset of saddlepoints in complex \mathbf{Q}_t -space [27]. By integrating Eq. (34) only along the steepest-descent contour through $\mathbf{Q}_t = \mathbf{Q}_t(\mathbf{t})$ rather than the entire set, we can isolate the desired ray contribution in a manner that is asymptotically equivalent to the SPA but is also well-behaved at caustics. (In this regard, we can also define the 'saddlepoint contribution' to an integral as the result of integrating along the corresponding steepest-descent contour.) Hence, the variable shift $\epsilon \doteq \mathbf{Q}_t - \mathbf{Q}_t(\mathbf{t})$ yields

$$\psi_t(\mathbf{q}) = \frac{\sigma_t \alpha_t \exp[-\frac{i}{2} \beta_t(\mathbf{q})]}{(-2\pi i)^{N/2} \sqrt{\det \mathbf{B}_t}} \Upsilon_t(\mathbf{q}), \quad (36)$$

where we have defined

$$\beta_t(\mathbf{q}) \doteq 2 G_t[\mathbf{q}, \mathbf{Q}_t(\mathbf{t})], \quad (37a)$$

$$\Upsilon_t(\mathbf{q}) \doteq \int_{\mathcal{C}_0} d\epsilon \Psi_t[\epsilon + \mathbf{Q}_t(\mathbf{t})] \exp[-i\gamma_t(\epsilon, \mathbf{q})], \quad (37b)$$

$$\gamma_t(\epsilon, \mathbf{q}) \doteq \frac{1}{2} \epsilon^\top \mathbf{D}_t \mathbf{B}_t^{-1} \epsilon + \epsilon^\top \mathbf{B}_t^{-\top} [\mathbf{D}_t^\top \mathbf{Q}_t(\mathbf{t}) - \mathbf{q}], \quad (37c)$$

and \mathcal{C}_0 is the steepest-descent contour through $\epsilon = \mathbf{0}$. Finally, $\psi(\mathbf{q})$ is reconstructed by summing over all branches of the dispersion manifold:

$$\psi(\mathbf{q}) = \sum_{\mathbf{t} \in \tau(\mathbf{q})} \psi_t[\mathbf{q}(\mathbf{t})]. \quad (38)$$

Equation (38) can accurately model the wavefield incident on an isolated fold caustic or bounded between a pair of fold caustics in 1-D. However, Eq. (38) cannot model a wavefield whose dispersion manifold has $\det \mathbf{B}_t = 0$ over a finite domain (examples of which are discussed in Sec. IV). We call such ray patterns 'quasi-uniform'. To enable MGO to model quasiuniform ray patterns, the restriction that $\det \mathbf{B}_t \neq 0$ must be lifted. The corresponding theory is discussed in the next section.

III. METAPLECTIC GEOMETRICAL OPTICS FOR QUASIUNIFORM RAY PATTERNS

A. Singular metaplectic transforms

The MT kernel $M(\mathbf{Q}, \mathbf{q}; \mathbf{S})$ that corresponds to a symplectic matrix \mathbf{S} with $\det \mathbf{B} = 0$ can be considered as a limiting case [14, 23]

$$M(\mathbf{Q}, \mathbf{q}; \mathbf{S}) = \lim_{\epsilon \rightarrow 0} M(\mathbf{Q}, \mathbf{q}; \mathbf{S}_\epsilon), \quad (39)$$

where \mathbf{S}_ϵ is a symplectic matrix that has \mathbf{S} as a limit as $\epsilon \rightarrow 0$. (Here and further, we omit the subscript \mathbf{t} for ease of notation.) For example, we can adopt

$$\mathbf{S}_\epsilon = \begin{pmatrix} \mathbf{A} & \mathbf{B} + \epsilon \mathbf{A} \\ \mathbf{C} & \mathbf{D} + \epsilon \mathbf{C} \end{pmatrix}, \quad (40)$$

whose symplecticity (to all orders in ϵ) can be readily verified by definition (15).

To show that $\det(\mathbf{B} + \epsilon \mathbf{A}) \neq 0$ and subsequently compute the limit in Eq. (39), it is useful to perform a singular value decomposition (SVD) of \mathbf{B} . Let ρ and $\varsigma \doteq N - \rho$ be the rank and corank of \mathbf{B} respectively. Then, the SVD of \mathbf{B} takes the form

$$\mathbf{B} = \mathbf{L} \tilde{\mathbf{B}} \mathbf{R}^\top, \quad (41)$$

where $\tilde{\mathbf{B}}$ is a diagonal matrix given by

$$\tilde{\mathbf{B}} = \begin{pmatrix} \Lambda_{\rho\rho} & 0_{\rho\varsigma} \\ 0_{\varsigma\rho} & 0_{\varsigma\varsigma} \end{pmatrix} \quad (42)$$

(the submatrices with subscript mn are size $m \times n$) and $\Lambda_{\rho\rho}$ is a diagonal matrix that has all nonzero singular values of \mathbf{B} on its diagonal:

$$\Lambda_{\rho\rho} \doteq \begin{pmatrix} \lambda_1 & & \\ & \ddots & \\ & & \lambda_\rho \end{pmatrix}. \quad (43)$$

Note that $\det \Lambda_{\rho\rho} \neq 0$ by definition. The matrices \mathbf{L} and \mathbf{R} are both orthogonal and can be written as

$$\mathbf{L} = \begin{pmatrix} \uparrow & & \uparrow \\ \check{\ell}_1 & \dots & \check{\ell}_N \\ \downarrow & & \downarrow \end{pmatrix}, \quad \mathbf{R} = \begin{pmatrix} \uparrow & & \uparrow \\ \check{\mathbf{r}}_1 & \dots & \check{\mathbf{r}}_N \\ \downarrow & & \downarrow \end{pmatrix}. \quad (44)$$

The columns of these matrices are, respectively, the left singular vectors $\{\check{\ell}_j\}$ and right singular vectors $\{\check{\mathbf{r}}_j\}$ of \mathbf{B} , which are mutually orthonormal:

$$\check{\ell}_j^\top \check{\ell}_k = \delta_{jk}, \quad \check{\mathbf{r}}_j^\top \check{\mathbf{r}}_k = \delta_{jk}. \quad (45)$$

Let us similarly define

$$\tilde{\mathbf{A}} \doteq \mathbf{L}^\top \mathbf{A} \mathbf{R}, \quad \tilde{\mathbf{C}} \doteq \mathbf{L}^\top \mathbf{C} \mathbf{R}, \quad \tilde{\mathbf{D}} \doteq \mathbf{L}^\top \mathbf{D} \mathbf{R}. \quad (46)$$

As shown in Appendix A, these matrices have the form

$$\tilde{\mathbf{A}} = \begin{pmatrix} a_{\rho\rho} & a_{\rho\varsigma} \\ 0_{\varsigma\rho} & a_{\varsigma\varsigma} \end{pmatrix}, \quad \tilde{\mathbf{C}} = \begin{pmatrix} c_{\rho\rho} & c_{\rho\varsigma} \\ c_{\varsigma\rho} & c_{\varsigma\varsigma} \end{pmatrix}, \quad \tilde{\mathbf{D}} = \begin{pmatrix} d_{\rho\rho} & 0_{\rho\varsigma} \\ d_{\varsigma\rho} & a_{\varsigma\varsigma}^{-\top} \end{pmatrix}. \quad (47)$$

Note that $a_{\varsigma\varsigma}$ is invertible. Hence, we compute

$$\begin{aligned} \det(\mathbf{B} + \varepsilon \mathbf{A}) &= \det \begin{pmatrix} \Lambda_{\rho\rho} + \varepsilon a_{\rho\rho} & \varepsilon a_{\rho\varsigma} \\ 0_{\varsigma\rho} & \varepsilon a_{\varsigma\varsigma} \end{pmatrix} \\ &= \det(\Lambda_{\rho\rho} + \varepsilon a_{\rho\rho}) \det(\varepsilon a_{\varsigma\varsigma}) \\ &\approx \varepsilon^\varsigma \det \Lambda_{\rho\rho} \det a_{\varsigma\varsigma}, \end{aligned} \quad (48)$$

where we have used $\det \mathbf{L} = \det \mathbf{R} = 1$. Since $\det a_{\varsigma\varsigma} \neq 0$ and $\det \Lambda_{\rho\rho} \neq 0$ by definition, $\det(\mathbf{B} + \varepsilon \mathbf{A})$ is nonzero for finite ε . (We adopt the convention that 0×0 matrices have unit determinant.)

By Eqs. (17) and (48), we obtain to leading order in ε

$$\begin{aligned} M(\mathbf{Q}, \mathbf{q}; \mathbf{S}_\varepsilon) &\approx \frac{\sigma \varepsilon^{-\varsigma/2} \exp[i g(\mathbf{q}_\rho, \mathbf{Q})]}{(2\pi i)^{N/2} \sqrt{\det \Lambda_{\rho\rho} \det a_{\varsigma\varsigma}}} \\ &\quad \times \exp\left(\frac{i}{2\varepsilon} |\mathbf{q}_\varsigma - a_{\varsigma\varsigma}^{-1} \mathbf{Q}_\varsigma|^2\right), \end{aligned} \quad (49)$$

where we have defined

$$\begin{aligned} g(\mathbf{q}_\rho, \mathbf{Q}) &\doteq \frac{1}{2} \mathbf{q}_\rho^\top \Lambda_{\rho\rho}^{-1} a_{\rho\rho} \mathbf{q}_\rho - \mathbf{q}_\rho^\top \mathbf{M}_1 \mathbf{L}^\top \mathbf{Q} \\ &\quad + \frac{1}{2} \mathbf{Q}^\top \mathbf{L} \mathbf{M}_2 \mathbf{L}^\top \mathbf{Q}, \end{aligned} \quad (50)$$

along with the matrices

$$\mathbf{M}_1 \doteq (\Lambda_{\rho\rho}^{-1} - \Lambda_{\rho\rho}^{-1} a_{\rho\varsigma} a_{\varsigma\varsigma}^{-1}), \quad (51a)$$

$$\mathbf{M}_2 \doteq \begin{pmatrix} d_{\rho\rho} \Lambda_{\rho\rho}^{-1} & \Lambda_{\rho\rho}^{-1} d_{\varsigma\rho}^\top \\ d_{\varsigma\rho} \Lambda_{\rho\rho}^{-1} & c_{\varsigma\varsigma} a_{\varsigma\varsigma}^{-1} - d_{\varsigma\rho} \Lambda_{\rho\rho}^{-1} a_{\rho\varsigma} a_{\varsigma\varsigma}^{-1} \end{pmatrix} \quad (51b)$$

and the vector decompositions

$$\mathbf{R}^\top \mathbf{q} = \begin{pmatrix} \mathbf{q}_\rho \\ \mathbf{q}_\varsigma \end{pmatrix}, \quad \mathbf{L}^\top \mathbf{Q} = \begin{pmatrix} \mathbf{Q}_\rho \\ \mathbf{Q}_\varsigma \end{pmatrix}. \quad (52)$$

Note that \mathbf{M}_2 and $\Lambda_{\rho\rho}^{-1} a_{\rho\rho}$ are symmetric [Eqs. (A4), (A7), and (A16)]. Also note that \mathbf{M}_1 is size $\rho \times N$, \mathbf{M}_2 is size $N \times N$, and any vector \mathbf{v}_m is size $m \times 1$. [Appendix B provides details for the derivation of Eq. (49).] Then, using Eq. (39) along with

$$\begin{aligned} \lim_{\varepsilon \rightarrow 0} \varepsilon^{-\varsigma/2} \exp\left(\frac{i}{2\varepsilon} |\mathbf{q}_\varsigma - a_{\varsigma\varsigma}^{-1} \mathbf{Q}_\varsigma|^2\right) \\ = (2\pi i)^{\varsigma/2} \delta(\mathbf{q}_\varsigma - a_{\varsigma\varsigma}^{-1} \mathbf{Q}_\varsigma), \end{aligned} \quad (53)$$

we obtain the limit of the MT kernel at $\det \mathbf{B} \rightarrow 0$:

$$M(\mathbf{Q}, \mathbf{q}) = \frac{\sigma \exp[i g(\mathbf{q}_\rho, \mathbf{Q})] \delta(\mathbf{q}_\varsigma - a_{\varsigma\varsigma}^{-1} \mathbf{Q}_\varsigma)}{(2\pi i)^{\rho/2} \sqrt{\det \Lambda_{\rho\rho} \det a_{\varsigma\varsigma}}}, \quad (54)$$

where, for brevity, we no longer mention the dependence of M on the symplectic matrix explicitly.

Following straightforward delta-function manipulations, we obtain the inverse MT kernel when $\det \mathbf{B} = 0$:

$$M^{-1}(\mathbf{q}, \mathbf{Q}) = \frac{\sigma \exp[-i \tilde{g}(\mathbf{Q}_\rho, \mathbf{q})] \delta(\mathbf{Q}_\varsigma - a_{\varsigma\varsigma} \mathbf{q}_\varsigma)}{(-2\pi i)^{\rho/2} \sqrt{\det \Lambda_{\rho\rho} \det a_{\varsigma\varsigma}^{-1}}}, \quad (55)$$

where we have defined

$$\begin{aligned} \tilde{g}(\mathbf{Q}_\rho, \mathbf{q}) &\doteq \frac{1}{2} \mathbf{Q}_\rho^\top d_{\rho\rho} \Lambda_{\rho\rho}^{-1} \mathbf{Q}_\rho - \mathbf{Q}_\rho^\top \mathbf{M}_3 \mathbf{R}^\top \mathbf{q} \\ &\quad + \frac{1}{2} \mathbf{q}^\top \mathbf{R} \mathbf{M}_4 \mathbf{R}^\top \mathbf{q}, \end{aligned} \quad (56)$$

along with the matrices

$$\mathbf{M}_3 \doteq (\Lambda_{\rho\rho}^{-1} - \Lambda_{\rho\rho}^{-1} d_{\varsigma\rho}^\top a_{\varsigma\varsigma}), \quad (57a)$$

$$\mathbf{M}_4 \doteq \begin{pmatrix} \Lambda_{\rho\rho}^{-1} a_{\rho\rho} & \Lambda_{\rho\rho}^{-1} a_{\rho\varsigma} \\ a_{\rho\varsigma}^\top \Lambda_{\rho\rho}^{-1} & a_{\rho\varsigma}^\top c_{\varsigma\varsigma} - a_{\rho\varsigma}^\top d_{\varsigma\rho} \Lambda_{\rho\rho}^{-1} a_{\rho\varsigma} \end{pmatrix}. \quad (57b)$$

Note that \mathbf{M}_4 and $d_{\rho\rho} \Lambda_{\rho\rho}^{-1}$ are symmetric [Eqs. (A4), (A7), and (A16)]. Also, \mathbf{M}_3 is size $\rho \times N$ while \mathbf{M}_4 is size $N \times N$. Lastly, we choose the following branch-cut convention: $\arg(i) = \pi/2$ and $\arg(\det \Lambda_{\rho\rho} \det a_{\varsigma\varsigma}) \in (-\pi, \pi]$ in Eq. (54); $\arg(-i) = -\pi/2$ and $\arg(\det \Lambda_{\rho\rho} \det a_{\varsigma\varsigma}^{-1}) \in [-\pi, \pi)$ in Eq. (55).

B. Singular metaplectic geometrical optics

Let us now incorporate the general representation for the inverse MT given by Eq. (55) into the MGO formalism. We emphasize that Eq. (55) is valid for all values of $\det \mathbf{B}$. Using Eqs. (34), (52), and (55) yields

$$\begin{aligned} \psi_{\mathbf{t}}(\mathbf{q}) &= \mathcal{N}_{\mathbf{t}}(\mathbf{q}) \int d\mathbf{Q}_\rho d\mathbf{Q}_\varsigma \delta(\mathbf{Q}_\varsigma - a_{\varsigma\varsigma} \mathbf{q}_\varsigma) \Psi_{\mathbf{t}} \left[\mathbf{L} \begin{pmatrix} \mathbf{Q}_\rho \\ \mathbf{Q}_\varsigma \end{pmatrix} \right] \\ &\quad \times \exp\left(-\frac{i}{2} \mathbf{Q}_\rho^\top d_{\rho\rho} \Lambda_{\rho\rho}^{-1} \mathbf{Q}_\rho + i \mathbf{Q}_\rho^\top \mathbf{M}_4 \mathbf{R}^\top \mathbf{q}\right), \end{aligned} \quad (58)$$

where we have substituted \mathbf{Q} with \mathbf{Q}_ρ and \mathbf{Q}_ς as

$$\mathbf{Q} = \mathbf{L} \begin{pmatrix} \mathbf{Q}_\rho \\ \mathbf{Q}_\varsigma \end{pmatrix}, \quad d\mathbf{Q} = d(\mathbf{L}\mathbf{Q}) = d\mathbf{Q}_\rho d\mathbf{Q}_\varsigma \quad (59)$$

and defined the prefactor

$$\mathcal{N}_t(\mathbf{q}) \doteq \frac{\sigma_t \alpha_t \exp\left(-\frac{i}{2} \mathbf{q}^\top \mathbf{R} \mathbf{M}_4 \mathbf{R}^\top \mathbf{q}\right)}{(-2\pi i)^{\rho/2} \sqrt{\det \Lambda_{\rho\rho} \det \mathbf{a}_{\varsigma\varsigma}^{-1}}}. \quad (60)$$

(As a reminder, all matrices depend on \mathbf{t} .) The integration over \mathbf{Q}_ς is immediately performed to yield

$$\begin{aligned} \psi_t(\mathbf{q}) &= \mathcal{N}_t(\mathbf{q}) \int d\mathbf{Q}_\rho \Psi_t \left[\mathbf{L} \begin{pmatrix} \mathbf{Q}_\rho \\ \mathbf{a}_{\varsigma\varsigma} \mathbf{q}_\varsigma \end{pmatrix} \right] \\ &\times \exp \left(-\frac{i}{2} \mathbf{Q}_\rho^\top d_{\rho\rho} \Lambda_{\rho\rho}^{-1} \mathbf{Q}_\rho + i \mathbf{Q}_\rho^\top \mathbf{M}_3 \mathbf{R}^\top \mathbf{q} \right). \end{aligned} \quad (61)$$

The phase of the integrand is stationary where

$$\partial_{\mathbf{Q}_\rho} \Theta_t \left[\mathbf{L} \begin{pmatrix} \mathbf{Q}_\rho \\ \mathbf{a}_{\varsigma\varsigma} \mathbf{q}_\varsigma \end{pmatrix} \right] + \mathbf{M}_3 \mathbf{R}^\top \mathbf{q} - d_{\rho\rho} \Lambda_{\rho\rho}^{-1} \mathbf{Q}_\rho = \mathbf{0}. \quad (62)$$

When \mathbf{q} is evaluated at the ray location $\mathbf{q}(t)$ in Eq. (38), then, using Eqs. (24), we can simplify

$$\begin{aligned} \mathbf{M}_3 \mathbf{R}^\top \mathbf{q}(t) &= \mathbf{M}_3 \mathbf{R}^\top \mathbf{D}^\top \mathbf{Q}_t(t) - \mathbf{M}_3 \mathbf{R}^\top \mathbf{B}^\top \mathbf{K}_t(t) \\ &= \Lambda_{\rho\rho}^{-1} d_{\rho\rho}^\top \mathbf{Q}_t^\rho(t) - \mathbf{K}_t^\rho(t), \end{aligned} \quad (63)$$

where we have defined the vector projections

$$\mathbf{L}^\top \mathbf{K}_t(t) \doteq \begin{pmatrix} \mathbf{K}_t^\rho(t) \\ \mathbf{K}_t^\varsigma(t) \end{pmatrix}, \quad (64a)$$

$$\mathbf{L}^\top \mathbf{Q}_t(t) \doteq \begin{pmatrix} \mathbf{Q}_t^\rho(t) \\ \mathbf{Q}_t^\varsigma(t) \end{pmatrix} = \begin{pmatrix} \mathbf{Q}_t^\rho(t) \\ \mathbf{a}_{\varsigma\varsigma} \mathbf{q}_\varsigma(t) \end{pmatrix}. \quad (64b)$$

Note that Eq. (64b) follows from Eq. (24). Since

$$\begin{aligned} \partial_{\mathbf{Q}_\rho} \Theta_t \left[\mathbf{L} \begin{pmatrix} \mathbf{Q}_\rho \\ \mathbf{a}_{\varsigma\varsigma} \mathbf{q}_\varsigma \end{pmatrix} \right] &= \begin{pmatrix} \leftarrow \check{\ell}_1^\top \rightarrow \\ \vdots \\ \leftarrow \check{\ell}_\rho^\top \rightarrow \end{pmatrix} \mathbf{K}_t \left[\mathbf{L} \begin{pmatrix} \mathbf{Q}_\rho \\ \mathbf{a}_{\varsigma\varsigma} \mathbf{q}_\varsigma \end{pmatrix} \right] \\ &\doteq \mathbf{K}_t^\rho \left[\mathbf{L} \begin{pmatrix} \mathbf{Q}_\rho \\ \mathbf{a}_{\varsigma\varsigma} \mathbf{q}_\varsigma \end{pmatrix} \right], \end{aligned} \quad (65)$$

the saddlepoint criterion (62) therefore becomes

$$\begin{aligned} \left\{ \mathbf{K}_t^\rho \left[\mathbf{L} \begin{pmatrix} \mathbf{Q}_\rho \\ \mathbf{a}_{\varsigma\varsigma} \mathbf{q}_\varsigma(t) \end{pmatrix} \right] - \mathbf{K}_t^\rho(t) \right\} \\ + d_{\rho\rho} \Lambda_{\rho\rho}^{-1} \left[\mathbf{Q}_t^\rho(t) - \mathbf{Q}_\rho \right] = \mathbf{0}, \end{aligned} \quad (66)$$

where we have used the fact that $d_{\rho\rho} \Lambda_{\rho\rho}^{-1}$ is symmetric.

As can be verified, the desired point \mathbf{t} on the dispersion manifold is a root to Eq. (66), since both terms in brackets vanish simultaneously when $\mathbf{Q}_\rho = \mathbf{Q}_t^\rho(t)$. Let us therefore define the new integration variable

$$\epsilon_\rho \doteq \mathbf{Q}_\rho - \mathbf{Q}_t^\rho(t), \quad d\epsilon_\rho = d\mathbf{Q}_\rho. \quad (67)$$

This yields a modified version of Eq. (36):

$$\psi_t(\mathbf{q}) = \frac{\sigma_t \alpha_t \exp\left[-\frac{i}{2} \beta_t^\rho(\mathbf{q})\right]}{(-2\pi i)^{\rho/2} \sqrt{\det \Lambda_{\rho\rho} \det \mathbf{a}_{\varsigma\varsigma}^{-1}}} \Upsilon_t^\rho(\mathbf{q}), \quad (68)$$

where we have defined

$$\beta_t^\rho(\mathbf{q}) \doteq 2 \tilde{g}_t[\mathbf{Q}_t^\rho(t), \mathbf{q}], \quad (69a)$$

$$\begin{aligned} \Upsilon_t^\rho(\mathbf{q}) &\doteq \int_{\mathcal{C}_0} d\epsilon_\rho \Psi_t \left[\mathbf{L} \begin{pmatrix} \mathbf{Q}_t^\rho(t) + \epsilon_\rho \\ \mathbf{a}_{\varsigma\varsigma} \mathbf{q}_\varsigma \end{pmatrix} \right] \\ &\times \exp[-i\gamma_t^\rho(\epsilon_\rho, \mathbf{q})], \end{aligned} \quad (69b)$$

$$\begin{aligned} \gamma_t^\rho(\epsilon_\rho, \mathbf{q}) &\doteq \frac{1}{2} \epsilon_\rho^\top d_{\rho\rho} \Lambda_{\rho\rho}^{-1} \epsilon_\rho \\ &+ \epsilon_\rho^\top [d_{\rho\rho} \Lambda_{\rho\rho}^{-1} \mathbf{Q}_t^\rho(t) - \mathbf{M}_3 \mathbf{R}^\top \mathbf{q}]. \end{aligned} \quad (69c)$$

Note that $\Upsilon_t^\rho(\mathbf{q})$ is integrated along the steepest-descent contour \mathcal{C}_0 passing through $\epsilon_\rho = \mathbf{0}$. Equation (38) with ψ_t computed via Eq. (68) constitutes the generalization of MGO to all values of $\det \mathbf{B}$. Thus, MGO can now be applied to any ray pattern in arbitrary media.

C. Metaplectic geometrical optics with Gaussian coherent states

Instead of performing an SVD of \mathbf{B} , we can develop an expression equivalent to Eq. (68) using

$$f(\mathbf{Q}, \mathbf{Z}_0) \doteq \exp \left[-\frac{|\mathbf{Q} - \mathbf{Q}_0|^2}{2} - i \mathbf{K}_0^\top \left(\mathbf{Q} - \frac{\mathbf{Q}_0}{2} \right) \right]. \quad (70)$$

These functions, which satisfy the completeness relation

$$\delta(\mathbf{Q} - \mathbf{Q}') = \int \frac{d\mathbf{Q}_0 d\mathbf{K}_0}{(2\pi)^N \pi^{N/2}} f(\mathbf{Q}, \mathbf{Z}_0) [f(\mathbf{Q}', \mathbf{Z}_0)]^*, \quad (71)$$

can be understood as the spatial representations of the Gaussian coherent states centered around $\mathbf{Z}_0 \doteq (\mathbf{Q}_0, \mathbf{K}_0)$ in phase space. These states are commonly used in quantum optics [28] and are discussed in detail in Appendix C and supplementary material. As shown in Appendix C, the property (71) ultimately leads to an alternate representation of the MT:

$$M_t^{-1}(\mathbf{q}, \mathbf{Q}) = \int d\mathbf{K}_0 \frac{\sigma \exp[\tilde{G}_t(\mathbf{q}, \boldsymbol{\xi}) - |\mathbf{K}_0|^2]}{(\sqrt{2\pi})^N \sqrt{\det(2\mathbf{D}_t - i\mathbf{B}_t)}}, \quad (72)$$

where we have defined $\boldsymbol{\xi} \doteq \mathbf{Q} + 2i\mathbf{K}_0$ and

$$\begin{aligned} \tilde{G}_t(\mathbf{q}, \boldsymbol{\xi}) &\doteq -\frac{1}{2} \mathbf{q}^\top (2\mathbf{D}_t - i\mathbf{B}_t)^{-1} (\mathbf{A}_t + 2i\mathbf{C}_t) \mathbf{q} \\ &+ \left(\mathbf{q} - \frac{1}{2} \mathbf{D}_t^\top \boldsymbol{\xi} \right)^\top (2\mathbf{D}_t - i\mathbf{B}_t)^{-1} \boldsymbol{\xi}. \end{aligned} \quad (73)$$

Note that the complex matrix $2\mathbf{D} - i\mathbf{B}$ is always invertible [29].

With Eq. (72) as the MT kernel, the phase of Eq. (34) is stationary where \mathbf{Q} and \mathbf{K}_0 simultaneously satisfy

$$2iD_t^\top [\mathbf{K}_t(\mathbf{Q}) - \mathbf{K}_0] + \mathbf{q} - D_t^\top \mathbf{Q} + B_t^\top \mathbf{K}_t(\mathbf{Q}) = 0, \quad (74a)$$

$$\mathbf{q} - D_t^\top \mathbf{Q} + B_t^\top \mathbf{K}_0 = 0. \quad (74b)$$

When \mathbf{q} is evaluated at $\mathbf{q}(\mathbf{t})$, a simultaneous solution to Eqs. (74) is $\mathbf{Q} = \mathbf{Q}_t(\mathbf{t})$ and $\mathbf{K}_0 = \mathbf{K}_t(\mathbf{t})$. Therefore, upon defining the new integration variables

$$\boldsymbol{\epsilon}_r \doteq \mathbf{Q} - \mathbf{Q}_t(\mathbf{t}), \quad \boldsymbol{\epsilon}_i \doteq 2\mathbf{K}_0 - 2\mathbf{K}_t(\mathbf{t}), \quad (75)$$

we obtain the following alternate representation of $\psi_t(\mathbf{q})$:

$$\begin{aligned} \psi_t(\mathbf{q}) &= \frac{\sigma_t \alpha_t \exp\{\tilde{G}_t[\mathbf{q}, \boldsymbol{\xi}_t(\mathbf{t})] - |\mathbf{K}_t(\mathbf{t})|^2\}}{(2\sqrt{2}\pi)^N \sqrt{\det(2D_t - iB_t)}} \\ &\times \int_{c_0} d\boldsymbol{\epsilon}_r d\boldsymbol{\epsilon}_i \Psi_t[\boldsymbol{\epsilon}_r + \mathbf{Q}_t(\mathbf{t})] \exp[-\tilde{\gamma}_t(\boldsymbol{\epsilon}, \mathbf{q}, \mathbf{t})], \quad (76) \end{aligned}$$

where we have defined

$$\boldsymbol{\epsilon} \doteq \boldsymbol{\epsilon}_r + i\boldsymbol{\epsilon}_i, \quad (77a)$$

$$\boldsymbol{\xi}_t(\mathbf{t}) \doteq \mathbf{Q}_t(\mathbf{t}) + 2i\mathbf{K}_t(\mathbf{t}), \quad (77b)$$

$$\begin{aligned} \tilde{\gamma}_t(\boldsymbol{\epsilon}, \mathbf{q}, \mathbf{t}) &\doteq \frac{1}{2} \boldsymbol{\epsilon}^\top D_t (2D_t - iB_t)^{-1} \boldsymbol{\epsilon} + \frac{|\boldsymbol{\epsilon}_i|^2}{4} + \boldsymbol{\epsilon}_i^\top \mathbf{K}_t(\mathbf{t}) \\ &- \boldsymbol{\epsilon}^\top (2D_t - iB_t)^{-\top} [\mathbf{q} - D_t^\top \boldsymbol{\xi}_t(\mathbf{t})]. \quad (77c) \end{aligned}$$

Equation (76) is equivalent to Eq. (68) but might be advantageous since it can be applied ‘as is’ without performing an SVD of B_t . That said, Eq. (76) involves a $2N$ -D integral, which is harder to evaluate numerically. In this sense, the representation (68) may be more practical, especially at large N .

IV. EXAMPLES

Here, we consider several examples of MGO, which have been shortened for clarity. The complete calculations can be found in the supplementary material.

A. Plane wave in uniform medium: No caustic

As a first example, let us consider a plane wave propagating in a uniform medium. For simplicity, we consider 1-D propagation governed by the one-way wave equation

$$i\partial_q \psi(q) + \psi(q) = 0. \quad (78)$$

There is no caustic in this case, and Eq. (78) is easy to integrate even without using MGO. However, this example is instructive to illustrate the reformulated MGO machinery when $\det B_t = 0$ with relatively little algebra.

Let us start by writing Eq. (78) in the integral form (1). The corresponding kernel $D(q, q')$ can be written as

$$D(q, q') = i\partial_{q'} \delta(q - q') - \delta(q - q'), \quad (79)$$

so the Weyl symbol (2) is as follows:

$$\mathcal{D}(q, k) = k - 1. \quad (80)$$

The corresponding ray equations are

$$\partial_\tau q(\tau) = 1, \quad \partial_\tau k(\tau) = 0, \quad (81)$$

with solutions given by

$$q(\tau) = \tau, \quad k(\tau) = 1, \quad (82)$$

where the integration constants have been chosen to satisfy $\mathcal{D}[q(0), k(0)] = 0$. Since $\tau(q) = q$ is single-valued, $\psi(q)$ will be absent of caustics.

From Eq. (81), it is clear that the tangent plane of the dispersion manifold is \mathbf{q} -space itself, that is,

$$S_t = I_2 \quad (83)$$

for all $t \in \tau(q)$. Hence, $\Psi_t(Q_t)$ is trivially obtained as

$$\Psi_t(Q_t) = \alpha_t \exp(iQ_t - it), \quad (84)$$

where we have used $Q_t(t) = t$. Since $\partial_t S_t = 0_2$, $\partial_Q \Psi_t(Q) = 0$, and $\partial_t Q_t(t) = 1$, we also compute

$$\eta_t = i, \quad \alpha_t = \alpha_0 \exp(it), \quad (85)$$

where α_0 is a constant. Then, since $B_t = 0$ implies that $\rho = 0$, $\varsigma = 1$, and $R = L = 1$, then $\beta_t^\rho = \gamma_t^\rho = 0$ and the integration over $d\epsilon_\rho$ is empty. Hence, Eq. (68) becomes

$$\psi_t[q(t)] = \sigma_t \alpha_0 \exp[iQ_t(t)]. \quad (86)$$

Since the branch cut of the MT is never crossed, we can take $\sigma_t = 1$. Then, the summation over branches is trivially performed to yield

$$\psi(q) = \sum_{t \in \tau(q)} \psi_t[q(t)] = \alpha_0 \exp(iq). \quad (87)$$

Equation (87) is an exact solution of Eq. (78), which is anticipated because (78) is a first-order equation and thus coincides with its GO approximation.

B. Plane wave in linearly stratified medium: Fold caustic

As a second example, let us consider oblique propagation in a linearly stratified medium. Suppose that the wave is described by the Helmholtz-type equation

$$\partial_{\mathbf{q}}^2 \psi(\mathbf{q}) + (k_0^2 - q_1) \psi(\mathbf{q}) = 0, \quad (88)$$

where k_0 is a constant and $\partial_{\mathbf{q}}^2 \doteq \partial_{q_1}^2 + \partial_{q_2}^2$. Our coordinate system is such that q_1 is aligned with the medium stratification and q_2 is transverse to q_1 . Let us also consider the initial condition

$$\psi(0, q_2) = c \exp(ik_0 q_2), \quad (89)$$

where c is an arbitrary constant.

Equation (88) can be equivalently written as an integral equation (1) with integration kernel

$$D(\mathbf{q}, \mathbf{q}') = -\partial_{\mathbf{q}}^2 \delta(\mathbf{q} - \mathbf{q}') + (q_1 - k_0^2) \delta(\mathbf{q} - \mathbf{q}'). \quad (90)$$

The corresponding Weyl symbol (2) is

$$D(\mathbf{q}, \mathbf{k}) = k_1^2 + k_2^2 + q_1 - k_0^2, \quad (91)$$

and the corresponding ray equations are

$$\partial_{\tau_1} q_1(\tau) = 2k_1(\tau), \quad \partial_{\tau_1} k_1(\tau) = -1, \quad (92a)$$

$$\partial_{\tau_1} q_2(\tau) = 2k_2(\tau), \quad \partial_{\tau_1} k_2(\tau) = 0. \quad (92b)$$

Let us define τ_1 such that $q_1(0, \tau_2) = 0$. Then, the initial condition (89) implies that $k_2(0, \tau_2) = k_0$, and the local dispersion relation $\mathcal{D}[\mathbf{q}(0, \tau_2), \mathbf{k}(0, \tau_2)] = 0$ requires $k_1(0, \tau_2) = 0$. This leaves $q_2(0, \tau_2)$ undetermined. Since τ_2 must parameterize the initial conditions for the rays, let us choose $q_2(0, \tau_2) = \tau_2$. Hence, the ray solutions are

$$q_1(\tau) = -\tau_1^2, \quad q_2(\tau) = \tau_2 + 2k_0\tau_1, \quad (93a)$$

$$k_1(\tau) = -\tau_1, \quad k_2(\tau) = k_0. \quad (93b)$$

The inverse function $\tau(\mathbf{q})$ is calculated as

$$\tau_1(\mathbf{q}) = \pm\sqrt{-q_1}, \quad \tau_2(\mathbf{q}) = q_2 \mp 2k_0\sqrt{-q_1}. \quad (94)$$

Clearly, $\tau(\mathbf{q})$ is double-valued, so there are two branches that must ultimately be summed over.

A basis for \mathbf{Q}_t -space is provided by the vector pair

$$\partial_{\tau_1} \mathbf{z}(\mathbf{t}) = (-2t_1 \ 2k_0 \ -1 \ 0)^\top, \quad (95a)$$

$$\partial_{\tau_2} \mathbf{z}(\mathbf{t}) = (0 \ 1 \ 0 \ 0)^\top, \quad (95b)$$

where $\mathbf{z}(\mathbf{t}) \doteq (\mathbf{q}(\mathbf{t}), \mathbf{k}(\mathbf{t}))^\top$. Then, symplectic Gram-Schmidt orthogonalization [15] yields the submatrices

$$\mathbf{A}_t = \mathbf{D}_t = \frac{1}{\vartheta_t} \begin{pmatrix} -2t_1 & 0 \\ 0 & \vartheta_t \end{pmatrix}, \quad (96a)$$

$$\mathbf{B}_t = -\mathbf{C}_t = \frac{1}{\vartheta_t} \begin{pmatrix} -1 & 0 \\ 0 & 0 \end{pmatrix}, \quad (96b)$$

where we have defined

$$\vartheta_t \doteq \sqrt{1 + 4t_1^2}. \quad (97)$$

The rotated rays are calculated via Eq. (24) as

$$\mathbf{Q}_t(\tau) = \begin{pmatrix} \frac{2t_1\tau_1^2 + \tau_1}{\vartheta_t} \\ \tau_2 + 2k_0\tau_1 \end{pmatrix}, \quad \mathbf{K}_t(\tau) = \begin{pmatrix} \frac{2t_1\tau_1 - \tau_1^2}{\vartheta_t} \\ k_0 \end{pmatrix}. \quad (98)$$

We can therefore compute the inverse function $\tau(\mathbf{Q}_t)$, which is double-valued. Upon restricting $\mathbf{K}_t(\mathbf{Q}_t)$ to the correct branch, we obtain

$$K_{t,1}(\mathbf{Q}_t) = -\frac{Q_{t,1}}{2t_1} - \vartheta_t \frac{1 - \sqrt{1 + 8t_1\vartheta_t Q_{t,1}}}{8t_1^2}, \quad (99a)$$

$$K_{t,2}(\mathbf{Q}_t) = k_0. \quad (99b)$$

Then, the line integral of Eq. (29) is computed to yield

$$\Theta_t[\boldsymbol{\epsilon} + \mathbf{Q}_t(\mathbf{t})] = k_0\epsilon_2 + \frac{8t_1^4 - \vartheta_t^4}{8t_1^2\vartheta_t} \epsilon_1 - \frac{1}{4t_1} \epsilon_1^2 + \frac{(\vartheta_t^4 + 8t_1\vartheta_t\epsilon_1)^{3/2} - \vartheta_t^6}{96t_1^3}. \quad (100)$$

Using Eqs. (27) and (28), we next compute

$$\Phi_t[\boldsymbol{\epsilon} + \mathbf{Q}_t(\mathbf{t})] = \frac{\vartheta_t}{(\vartheta_t^4 + 8t_1\vartheta_t\epsilon_1)^{1/4}}, \quad (101)$$

where we have chosen the initial conditions to satisfy

$$\Phi_t[\mathbf{Q}_t(t_1, \tau_2)] = 1. \quad (102)$$

We then compute via Eqs. (31) and (32)

$$\alpha_t = \frac{\alpha_{(0,t_2)}}{\sqrt{\vartheta_t}} \exp\left(2ik_0^2t_1 + i\frac{2t_1^3}{3} - i\frac{t_1^5}{\vartheta_t^2}\right), \quad (103)$$

where $\alpha_{(0,t_2)}$ is an arbitrary initial condition.

We now perform the inverse MT. Note that \mathbf{B}_t is already in the desired SVD form, with $\mathbf{L} = \mathbf{R} = \mathbf{l}_2$ and $\rho = 1$. Since $\epsilon_\rho = \epsilon_1$ and $\mathbf{Q}_t^\rho(\mathbf{t}) = \mathbf{Q}_{t,1}(\mathbf{t})$, we compute

$$\beta_t^\rho[\mathbf{q}(\mathbf{t})] = -\frac{2t_1^5}{\vartheta_t^2}, \quad \gamma_t^\rho[\boldsymbol{\epsilon}_\rho, \mathbf{q}(\mathbf{t})] = \frac{t_1^2}{\vartheta_t} \epsilon_1 + t_1 \epsilon_1^2. \quad (104)$$

Hence, we obtain

$$\Upsilon_t^\rho[\mathbf{q}(\mathbf{t})] = \int_{\mathcal{C}_0} d\epsilon_1 \frac{\vartheta_t}{(\vartheta_t^4 + 8t_1\vartheta_t\epsilon_1)^{1/4}} \times \exp\left[i\frac{(\vartheta_t^4 + 8t_1\vartheta_t\epsilon_1)^{3/2} - \vartheta_t^6}{96t_1^3} - i\frac{\vartheta_t^2}{4t_1} \epsilon_1^2 - i\frac{\vartheta_t^3}{8t_1^2} \epsilon_1\right]. \quad (105)$$

This is the same integral that was studied in Ref. [15], where the following approximation was derived:

$$\Upsilon_t^\rho[\mathbf{q}(\mathbf{t})] \approx \pi\vartheta_t \exp\left(-i\frac{2}{3}t_1^3\vartheta_t^6\right) \times \left[\text{Ai}(-t_1^2\vartheta_t^4) - i\frac{t_1}{|t_1|} \text{Bi}(-t_1^2\vartheta_t^4)\right], \quad (106)$$

where $\text{Ai}(x)$ and $\text{Bi}(x)$ are the Airy functions of the first and second kind, respectively [30]. Thus, Eq. (68) yields

$$\psi_t[\mathbf{q}(\mathbf{t})] = i\sigma_t \alpha_{(0,t_2)} \frac{\vartheta_t \sqrt{\pi}}{\sqrt{-2i}} \exp\left[2ik_0^2t_1 + i\frac{2t_1^3}{3}(1 - \vartheta_t^6)\right] \times \left[\text{Ai}(-t_1^2\vartheta_t^4) - i\frac{t_1}{|t_1|} \text{Bi}(-t_1^2\vartheta_t^4)\right]. \quad (107)$$

Since the MT branch cut is never crossed, we can take $\sigma_t = 1$. Then, summing over both branches of $\tau(\mathbf{q})$ [Eq. (94)] and choosing

$$\alpha_{(0,t_2)} = \frac{\sqrt{-2i}}{2i\sqrt{\pi}} \exp(ik_0t_2) \quad (108)$$

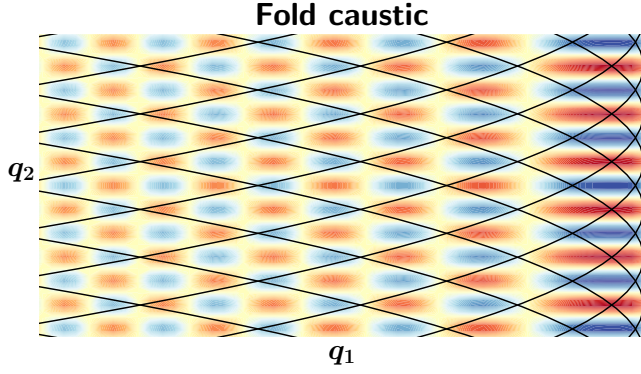


FIG. 1: Contour plot showing the real part of the MGO solution (109), with $k_0 = 2$, near the fold caustic (cutoff) located at $q_1 = 0$ (magenta). The ray trajectories $(q_1(\tau), q_2(\tau))$ are shown as black curves. Note that the field remains finite along the caustic. In fact, the MGO solution is nearly indistinguishable with the exact solution (111).

to satisfy the initial condition (89) ultimately yields

$$\psi(\mathbf{q}) = \sqrt{1 - 4q_1} \exp(ik_0q_2) \times \left\{ \text{Ai}[-\varrho^2(q_1)] \cos \varpi(q_1) - \text{Bi}[-\varrho^2(q_1)] \sin \varpi(q_1) \right\}, \quad (109)$$

where we have chosen $c = \text{Ai}(0)$ and defined

$$\varrho(q_1) \doteq (1 - 4q_1)\sqrt{-q_1}, \quad (110a)$$

$$\varpi(q_1) \doteq \frac{2}{3}\varrho^3(q_1) - \frac{2}{3}(-q_1)^{3/2}. \quad (110b)$$

The MGO solution (109) is plotted in Fig. 1. Notably, this solution is finite along the caustic surface (cutoff) located at $q_1 = 0$, and agrees remarkably well with the exact solution of Eq. (88),

$$\psi_{\text{ex}}(\mathbf{q}) = \text{Ai}(q_1) \exp(ik_0q_2). \quad (111)$$

A similar plot of Eq. (111) is not presented because it is virtually indistinguishable from Fig. 1.

C. Imperfectly focused plane wave in uniform medium: Cusp caustic

As a final example, let us consider a 2-D plane wave described by the paraxial wave equation [31]

$$i\partial_{q_1}\psi(\mathbf{q}) + \frac{1}{2}\partial_{q_2}^2\psi(\mathbf{q}) + \psi(\mathbf{q}) = 0, \quad (112)$$

where q_1 is aligned with the optical axis and q_2 is transverse to it. Let us assume the initial condition

$$\psi(0, q_2) = \sqrt{\frac{2\pi i}{f}} \exp\left(-\frac{i}{2f}q_2^2 - \frac{ia}{4f^3}q_2^4\right). \quad (113)$$

This corresponds to a wave that is being focused by an imperfect lens, with focal distance f and aberration a .

In the absence of aberration ($a = 0$), the initial field will focus at $\mathbf{q} = (f, 0)$; however, as shown in Fig. 2, finite aberration causes the focusing to become distorted, resulting in a cusped wavefield. For simplicity, we shall assume that $f \gg 1$ and $a < 0$.

Equation (112) can be equivalently written as an integral equation (1) with integration kernel

$$D(\mathbf{q}, \mathbf{q}') = i\partial_{q_1'}\delta(\mathbf{q} - \mathbf{q}') - \frac{1}{2}\partial_{q_2'}^2\delta(\mathbf{q} - \mathbf{q}') - \delta(\mathbf{q} - \mathbf{q}'). \quad (114)$$

The corresponding Weyl symbol (2) is

$$\mathcal{D}(\mathbf{q}, \mathbf{k}) = k_1 + \frac{k_2^2}{2} - 1, \quad (115)$$

and the corresponding ray equations are

$$\partial_{\tau_1}k_1(\tau) = 0, \quad \partial_{\tau_1}q_1(\tau) = 1, \quad (116a)$$

$$\partial_{\tau_1}k_2(\tau) = 0, \quad \partial_{\tau_1}q_2(\tau) = k_2(\tau). \quad (116b)$$

Similar to the previous example, let us define τ_1 and τ_2 such that $q_1(0, \tau_2) = 0$ and $q_2(0, \tau_2) = f\tau_2$. Then, imposing the local dispersion relation (4) and the initial condition (113) yields the ray trajectories

$$q_1(\tau) = \tau_1, \quad q_2(\tau) = f\tau_2 + k_2(\tau)\tau_1, \quad (117a)$$

$$k_1(\tau) = 1 - \frac{k_2^2(\tau)}{2}, \quad k_2(\tau) = -\tau_2 - a\tau_2^3. \quad (117b)$$

The inverse function $\tau(\mathbf{q})$ is either single- or triple-valued, depending on the value of the discriminant

$$\Delta(\mathbf{q}) = 4\left(\frac{q_1 - f}{aq_1}\right)^3 + 27\left(\frac{q_2}{aq_1}\right)^2. \quad (118)$$

If $\Delta(\mathbf{q}) > 0$, there is only one ray given by

$$\tau_2^{(0)}(\mathbf{q}) = \sqrt[3]{-\frac{q_2}{2aq_1} + \sqrt{\frac{\Delta(\mathbf{q})}{108}}} + \sqrt[3]{-\frac{q_2}{2aq_1} - \sqrt{\frac{\Delta(\mathbf{q})}{108}}}, \quad (119)$$

while if $\Delta(\mathbf{q}) \leq 0$, there are two additional rays given by

$$\tau_2^{(\pm)}(\mathbf{q}) = \text{Re} \left[(-1 \pm i\sqrt{3}) \sqrt[3]{-\frac{q_2}{2aq_1} + i\sqrt{\frac{|\Delta(\mathbf{q})|}{108}}} \right]. \quad (120)$$

For all values of $\Delta(\mathbf{q})$, one has $\tau_1(\mathbf{q}) = q_1$.

A basis for $\mathbf{Q}_{\mathbf{t}}$ -space is provided by the vector pair

$$\partial_{\tau_1}\mathbf{z}(\mathbf{t}) = (1 \quad k_2(\mathbf{t}) \quad 0 \quad 0)^\top, \quad (121a)$$

$$\partial_{\tau_2}\mathbf{z}(\mathbf{t}) = (0 \quad j_{\mathbf{t}} \quad -k_2(\mathbf{t})k_2'(\mathbf{t}) \quad k_2'(\mathbf{t}))^\top, \quad (121b)$$

where we have defined

$$j_{\mathbf{t}} \doteq \det \partial_{\tau}\mathbf{q}(\mathbf{t}) = f + t_1k_2'(\mathbf{t}). \quad (122)$$

Then, $\mathbf{S}_{\mathbf{t}}$ is constructed using symplectic Gram-Schmidt orthogonalization [15]. This yields the submatrices

$$\mathbf{A}_{\mathbf{t}} = \mathbf{D}_{\mathbf{t}} = \frac{1}{\vartheta_{\mathbf{t}}\varphi_{\mathbf{t}}} \begin{pmatrix} \varphi_{\mathbf{t}} & \varphi_{\mathbf{t}}k_2(\mathbf{t}) \\ -j_{\mathbf{t}}k_2(\mathbf{t}) & j_{\mathbf{t}} \end{pmatrix}, \quad (123a)$$

$$\mathbf{B}_{\mathbf{t}} = -\mathbf{C}_{\mathbf{t}} = \frac{\vartheta_{\mathbf{t}}k_2'(\mathbf{t})}{\varphi_{\mathbf{t}}} \begin{pmatrix} 0 & 0 \\ -k_2(\mathbf{t}) & 1 \end{pmatrix}, \quad (123b)$$

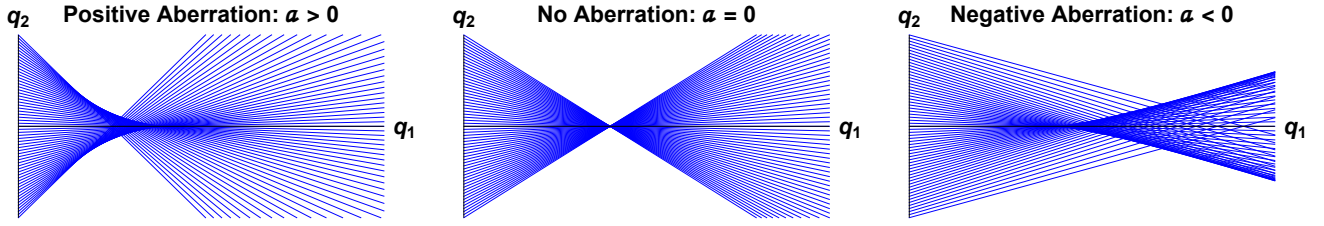


FIG. 2: Ray trajectories for the paraxial equation (112) with initial conditions given by Eq. (113). For no aberration ($a = 0$), the rays focus at $\mathbf{q} = (f, 0)$. Positive aberration ($a > 0$) causes the outer rays to focus before the focal point, while negative aberration ($a < 0$) causes the outer rays to focus beyond the focal point. Both cases result in a cusped ray pattern.

where we have defined

$$\vartheta_{\mathbf{t}} \doteq \sqrt{1 + k_2^2(\mathbf{t})}, \quad \varphi_{\mathbf{t}} \doteq \sqrt{j_{\mathbf{t}}^2 + [k_2'(\mathbf{t})\vartheta_{\mathbf{t}}^2]^2}. \quad (124)$$

The rotated rays are computed using Eqs. (24), although the result is quite lengthy and will not be shown. Next, using Eq. (27) we compute the envelope as

$$\Phi_{\mathbf{t}}(\tau) = \frac{\varphi_{\mathbf{t}}}{\sqrt{j_{\mathbf{t}}j_{\tau} + [1 + k_2(\mathbf{t})k_2(\tau)]^2 k_2'(\tau)k_2'(\mathbf{t})}}, \quad (125)$$

where $\Phi_{\mathbf{t}}(\tau) \doteq \Phi_{\mathbf{t}}[\mathbf{Q}_{\mathbf{t}}(\tau)]$ and we have chosen

$$\Phi_{\mathbf{t}}[\mathbf{Q}_{\mathbf{t}}(t_1, \tau_2)] = 1. \quad (126)$$

Although $\tau(\mathbf{Q}_{\mathbf{t}})$ is impractical to construct explicitly, $\partial_{\mathbf{Q}}\Phi_{\mathbf{t}}$ can still be calculated from $\Phi_{\mathbf{t}}(\tau)$ using

$$\partial_{\mathbf{Q}}\Phi_{\mathbf{t}}[\mathbf{Q}_{\mathbf{t}}(\mathbf{t})] = [\partial_{\tau}\mathbf{Q}_{\mathbf{t}}(\mathbf{t})]^{-1} \partial_{\tau}\Phi_{\mathbf{t}}(\mathbf{t}). \quad (127)$$

Ultimately, Eqs. (31) and (32) yield

$$\alpha_{\mathbf{t}} = \alpha_{(0,t_2)} \sqrt{\frac{\varphi_{(0,t_2)}}{\varphi_{\mathbf{t}}}} \exp \left\{ it_1 \frac{1 + \vartheta_{\mathbf{t}}^2}{2} + \frac{i}{2} \beta_{\mathbf{t}}^{\rho}[\mathbf{q}(\mathbf{t})] - \frac{i}{2} \beta_{(0,t_2)}^{\rho}[\mathbf{q}(0, t_2)] \right\}, \quad (128)$$

where $\alpha_{(0,t_2)}$ is determined by the initial conditions and $\beta_{\mathbf{t}}^{\rho}[\mathbf{q}(\mathbf{t})]$ is defined below [Eq. (130a)].

We next perform an SVD of $\mathbf{B}_{\mathbf{t}}$ to obtain

$$\mathbf{L} = \begin{pmatrix} 0 & 1 \\ -1 & 0 \end{pmatrix}, \quad \mathbf{R} = \frac{1}{\vartheta_{\mathbf{t}}} \begin{pmatrix} k_2(\mathbf{t}) & 1 \\ -1 & k_2(\mathbf{t}) \end{pmatrix}. \quad (129)$$

Hence, we can compute

$$\beta_{\mathbf{t}}^{\rho}[\mathbf{q}(\mathbf{t})] = \frac{f^2 j_{\mathbf{t}} t_2^2}{\vartheta_{\mathbf{t}}^4 k_2'(\mathbf{t})} - \frac{2f\varphi_{\mathbf{t}} t_2 Q_{\mathbf{t},2}(\mathbf{t})}{\vartheta_{\mathbf{t}}^3 k_2'(\mathbf{t})} + \frac{j_{\mathbf{t}} Q_{\mathbf{t},2}^2(\mathbf{t})}{\vartheta_{\mathbf{t}}^2 k_2'(\mathbf{t})}, \quad (130a)$$

$$\gamma_{\mathbf{t}}^{\rho}[\epsilon_{\rho}, \mathbf{q}(\mathbf{t})] = \frac{j_{\mathbf{t}}}{2\vartheta_{\mathbf{t}}^2 k_2'(\mathbf{t})} \epsilon_{\rho}^2 - K_{\mathbf{t},2}(\mathbf{t}) \epsilon_{\rho}. \quad (130b)$$

Thus, Eq. (68) yields

$$\psi_{\mathbf{t}}[\mathbf{q}(\mathbf{t})] = \frac{\sigma_{\mathbf{t}} \alpha_{(0,t_2)} \sqrt{\varphi_{(0,t_2)}}}{\vartheta_{\mathbf{t}} \sqrt{-2\pi i} \sqrt{k_2'(\mathbf{t})}} \Upsilon_{\mathbf{t}}^{\rho}[\mathbf{q}(\mathbf{t})] \times \exp \left\{ it_1 \frac{1 + \vartheta_{\mathbf{t}}^2}{2} - \frac{i}{2} \beta_{(0,t_2)}^{\rho}[\mathbf{q}(0, t_2)] \right\}. \quad (131)$$

Note that $k_2'(\mathbf{t})$ can change sign, meaning $\sigma_{\mathbf{t}} \neq 1$. However, we do not need to explicitly compute $\sigma_{\mathbf{t}}$ since it will be removed by matching to initial conditions.

After making a slow-envelope approximation, a quartic polynomial (normal form) can be fit to an implicit Taylor expansion of $\Theta_{\mathbf{t}}[Q_{\mathbf{t},1}(\mathbf{t}), Q_{\mathbf{t},2}(\mathbf{t}) - \epsilon_{\rho}]$ to ultimately yield

$$\Upsilon_{\mathbf{t}}^{\rho}[\mathbf{q}(\mathbf{t})] \approx \vartheta_{\mathbf{t}} \left| \frac{f}{a} \right|^{1/4} \sqrt{\frac{-2k_2'(\mathbf{t})}{t_1}} \exp \left(i \frac{j_{\mathbf{t}} + f - t_1}{4t_1} f t_2^2 \right) \times \int_{\mathcal{C}_{t_2}} d\varepsilon \exp(iy_{\mathbf{t}}\varepsilon + ix_{\mathbf{t}}\varepsilon^2 + i\varepsilon^4), \quad (132)$$

where we have defined

$$x_{\mathbf{t}} \doteq \left| \frac{f}{a} \right|^{1/2} \frac{f - q_1(\mathbf{t})}{q_1(\mathbf{t})}, \quad y_{\mathbf{t}} \doteq \left| \frac{4f^3}{a} \right|^{1/4} \frac{q_2(\mathbf{t})}{q_1(\mathbf{t})}, \quad (133)$$

and \mathcal{C}_{t_2} is the steepest-descent contour through the saddlepoint $\varepsilon = -t_2 |fa|^{1/4} / \sqrt{2}$.

Our assumption $a < 0$ implies that $\tau(\mathbf{q})$ is single-valued along the initial surface. Thus, Eq. (131) yields

$$\psi[\mathbf{q}(0, t_2)] = \sigma_{t_2} \alpha_{(0,t_2)} \sqrt{\frac{\varphi_{(0,t_2)}}{f}} \times \exp \left\{ i \frac{1 - s_{\mathbf{t}}}{2} \pi - \frac{i}{2} \beta_{(0,t_2)}^{\rho}[\mathbf{q}(0, t_2)] \right\}, \quad (134)$$

where we have defined $s_{\mathbf{t}} \doteq \text{sgn}[k_2'(\mathbf{t})]$ and have evaluated Eq. (132) in the GO limit, since $f \gg 1$ implies that the initial surface lies sufficiently far from the caustic. Thus, the initial conditions are satisfied by the choice

$$\alpha_{(0,t_2)} = \frac{\sqrt{2\pi}}{\sigma_{t_2} \sqrt{\varphi_{(0,t_2)}}} \exp \left\{ \frac{i}{2} \beta_{(0,t_2)}^{\rho}[\mathbf{q}(0, t_2)] - \frac{i}{2} f t_2^2 - \frac{ia}{4} f t_2^4 + i \frac{2s_{\mathbf{t}} - 1}{4} \pi \right\}. \quad (135)$$

Equation (38) therefore yields

$$\psi(\mathbf{q}) = \left| \frac{4f}{a q_1^2} \right|^{1/4} \exp \left(i q_1 + i \frac{q_2^2}{2q_1} \right) \times \sum_{t_2 \in \tau_2(\mathbf{q})} \int_{\mathcal{C}_{t_2}} d\varepsilon \exp(iy_{\mathbf{t}}\varepsilon + ix_{\mathbf{t}}\varepsilon^2 + i\varepsilon^4), \quad (136)$$

where the sum is over all real saddlepoint contributions.

Let us recall the Pearcey function [32], defined as

$$\text{Pe}(x, y) \doteq \int_{-\infty}^{\infty} ds \exp(iys + ix s^2 + is^4). \quad (137)$$

Then, when $\Delta(\mathbf{q})\tilde{\Delta}(\mathbf{q}) \geq 0$, where

$$\tilde{\Delta}(\mathbf{q}) \doteq 2 \left(\frac{f - q_1}{|a|q_1} \right)^3 + 27(5 - \sqrt{27}) \left(\frac{q_2}{|a|q_1} \right)^2, \quad (138)$$

the summation in Eq. (136) is simplified as

$$\sum_{t_2 \in \tau_2(\mathbf{q})} \int_{\mathcal{C}_{t_2}} d\varepsilon \exp(iy_t \varepsilon + ix_t \varepsilon^2 + i\varepsilon^4) = \text{Pe}(x_t, y_t). \quad (139)$$

When $\Delta(\mathbf{q})\tilde{\Delta}(\mathbf{q}) < 0$ (the caustic shadow), $\text{Pe}(x, y)$ contains an additional contribution from one of the two complex saddlepoints [33], which is not included in Eq. (136). It does not seem possible to isolate the real saddlepoint contribution to $\text{Pe}(x, y)$ using a complex rotation as done in Ref. [15] for $\text{Ai}(x)$. Nevertheless, the shadow contribution is asymptotically subdominant, so within the MGO accuracy we can include it such that Eq. (136) can be universally expressed through the Pearcey function as

$$\begin{aligned} \psi(\mathbf{q}) &= \left| \frac{4f}{aq_1^2} \right|^{1/4} \exp\left(iq_1 + i\frac{q_2^2}{2q_1}\right) \\ &\times \text{Pe}\left(\left| \frac{f}{a} \right|^{1/2} \frac{f - q_1}{q_1}, \left| \frac{4f^3}{a} \right|^{1/4} \frac{q_2}{q_1}\right). \end{aligned} \quad (140)$$

As readily verified, Eq. (140) also happens to be the exact solution of Eq. (112) for the initial condition (113). This solution is illustrated in Fig. 3 for $a = -4/f$.

V. CONCLUSION

Metaplectic geometrical optics, or MGO, has recently been developed to accurately model caustics by integrating field equations over GO rays. However, as originally formulated in Ref. [15], MGO fails to describe what we call quasiuniform ray patterns ($\det \mathbf{B}_t = 0$ over a finite domain). Here, we extend MGO so that the new theory can be applied to any ray pattern in both uniform and nonuniform media. To aid practical implementations, we provide two equivalent representations of the new MGO using either singular value decompositions or Gaussian states.

We demonstrate MGO analytically in three examples, namely, a plane wave propagating in uniform media (no caustic), a plane wave incident on an isolated cut-off (Airy-type fold caustic), and an imperfectly focused plane wave in vacuum (Pearcey-type cusp caustic). In all examples, MGO provides an accurate representation of the exact solution that remains finite at the caustics, unlike traditional GO. Yet, as the final example shows,

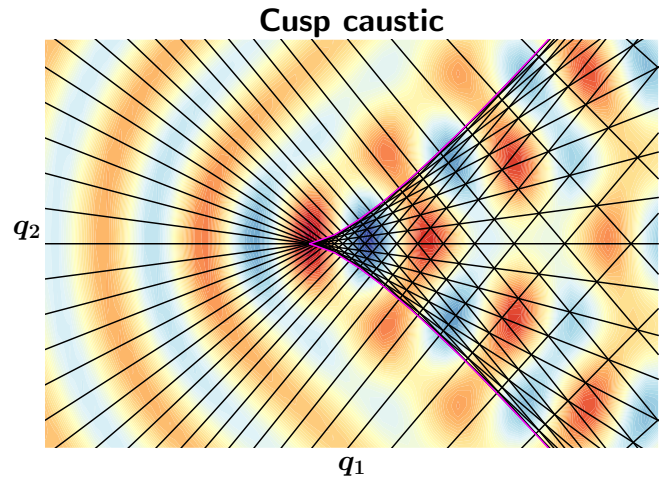


FIG. 3: Contour plot showing the real part of the MGO solution (140), with $a = -4/f$, near a cusp caustic located at $q_2 = \pm\sqrt{4(f - q_1)^3/27aq_1}$ (magenta). The ray trajectories $(q_1(\tau), q_2(\tau))$ are shown as black lines. Note that the field remains finite along the caustic.

MGO does not always accurately model caustic shadows. Further extensions of MGO to incorporate caustic shadow fields will be investigated in future research. In future work we shall also explore how to include polarization dynamics for modeling vector waves with MGO, including spin-orbit coupling [21, 34–42], mode conversion [21, 43–45], and optical anisotropy [36, 46–48].

ACKNOWLEDGEMENTS

The work was supported by the U.S. DOE through Contract No. DE-AC02-09CH11466.

Appendix A: Symplectic matrices in the SVD basis

As is well-known, the symplectic criterion (15) for \mathbf{S} implies that \mathbf{A} , \mathbf{B} , \mathbf{C} , and \mathbf{D} satisfy [14, 49]

$$\mathbf{A}\mathbf{B}^\top - \mathbf{B}\mathbf{A}^\top = \mathbf{0}_N, \quad (\text{A1a})$$

$$\mathbf{B}^\top\mathbf{D} - \mathbf{D}^\top\mathbf{B} = \mathbf{0}_N, \quad (\text{A1b})$$

$$\mathbf{A}\mathbf{D}^\top - \mathbf{B}\mathbf{C}^\top = \mathbf{I}_N, \quad (\text{A1c})$$

$$\mathbf{A}^\top\mathbf{D} - \mathbf{C}^\top\mathbf{B} = \mathbf{I}_N, \quad (\text{A1d})$$

$$\mathbf{C}^\top\mathbf{A} - \mathbf{A}^\top\mathbf{C} = \mathbf{0}_N, \quad (\text{A1e})$$

$$\mathbf{D}\mathbf{C}^\top - \mathbf{C}\mathbf{D}^\top = \mathbf{0}_N. \quad (\text{A1f})$$

The orthogonality of \mathbf{L} and \mathbf{R} means that $\tilde{\mathbf{A}}$, $\tilde{\mathbf{B}}$, $\tilde{\mathbf{C}}$, and $\tilde{\mathbf{D}}$ also satisfy Eqs. (A1). After using the parameterization

$$\tilde{\mathbf{A}} = \begin{pmatrix} \mathbf{a}_{\rho\rho} & \mathbf{a}_{\rho\varsigma} \\ \mathbf{a}_{\varsigma\rho} & \mathbf{a}_{\varsigma\varsigma} \end{pmatrix} \quad (\text{A2})$$

(where each block \mathbf{a}_{mn} is a matrix of size $m \times n$),

Eq. (A1a) reads

$$\begin{pmatrix} \mathbf{a}_{\rho\rho}\Lambda_{\rho\rho} - (\mathbf{a}_{\rho\rho}\Lambda_{\rho\rho})^\top & -(\mathbf{a}_{\varsigma\rho}\Lambda_{\rho\rho})^\top \\ \mathbf{a}_{\varsigma\rho}\Lambda_{\rho\rho} & \mathbf{0}_{\varsigma\varsigma} \end{pmatrix} = \mathbf{0}_N. \quad (\text{A3})$$

Since $\Lambda_{\rho\rho} \neq \mathbf{0}_{\rho\rho}$, this implies that

$$\mathbf{a}_{\varsigma\rho} = \mathbf{0}_{\varsigma\rho}, \quad \mathbf{a}_{\rho\rho}\Lambda_{\rho\rho} = (\mathbf{a}_{\rho\rho}\Lambda_{\rho\rho})^\top. \quad (\text{A4})$$

Similarly, after using the parameterization

$$\tilde{\mathbf{D}} = \begin{pmatrix} \mathbf{d}_{\rho\rho} & \mathbf{d}_{\rho\varsigma} \\ \mathbf{d}_{\varsigma\rho} & \mathbf{d}_{\varsigma\varsigma} \end{pmatrix}, \quad (\text{A5})$$

Eq. (A1b) becomes

$$\begin{pmatrix} \Lambda_{\rho\rho}\mathbf{d}_{\rho\rho} - (\Lambda_{\rho\rho}\mathbf{d}_{\rho\rho})^\top & \Lambda_{\rho\rho}\mathbf{d}_{\rho\varsigma} \\ -(\Lambda_{\rho\rho}\mathbf{d}_{\rho\varsigma})^\top & \mathbf{0}_{\varsigma\varsigma} \end{pmatrix} = \mathbf{0}_N. \quad (\text{A6})$$

This yields analogous constraints on $\tilde{\mathbf{D}}$, namely

$$\mathbf{d}_{\rho\varsigma} = \mathbf{0}_{\rho\varsigma}, \quad \Lambda_{\rho\rho}\mathbf{d}_{\rho\rho} = (\Lambda_{\rho\rho}\mathbf{d}_{\rho\rho})^\top. \quad (\text{A7})$$

Next, after using the parameterization

$$\tilde{\mathbf{C}} = \begin{pmatrix} \mathbf{c}_{\rho\rho} & \mathbf{c}_{\rho\varsigma} \\ \mathbf{c}_{\varsigma\rho} & \mathbf{c}_{\varsigma\varsigma} \end{pmatrix}, \quad (\text{A8})$$

Eq. (A1c) becomes

$$\begin{pmatrix} \mathbf{a}_{\rho\rho}\mathbf{d}_{\rho\rho}^\top - \Lambda_{\rho\rho}\mathbf{c}_{\rho\rho}^\top & \mathbf{a}_{\rho\rho}\mathbf{d}_{\varsigma\rho}^\top + \mathbf{a}_{\rho\varsigma}\mathbf{d}_{\varsigma\varsigma}^\top - \Lambda_{\rho\rho}\mathbf{c}_{\varsigma\rho}^\top \\ \mathbf{0}_{\varsigma\rho} & \mathbf{a}_{\varsigma\varsigma}\mathbf{d}_{\varsigma\varsigma}^\top \end{pmatrix} = \mathbf{I}_N. \quad (\text{A9})$$

Since the matrix inverse is unique, we therefore obtain

$$\mathbf{d}_{\varsigma\varsigma} = \mathbf{a}_{\varsigma\varsigma}^{-\top}, \quad (\text{A10})$$

which means that $\mathbf{a}_{\varsigma\varsigma}$ is invertible. Since $\Lambda_{\rho\rho}$ is invertible, we also obtain

$$\mathbf{c}_{\rho\rho} = \mathbf{d}_{\rho\rho}\mathbf{a}_{\rho\rho}^\top\Lambda_{\rho\rho}^{-1} - \Lambda_{\rho\rho}^{-1}, \quad (\text{A11a})$$

$$\mathbf{c}_{\varsigma\rho} = \mathbf{d}_{\varsigma\rho}\mathbf{a}_{\rho\rho}^\top\Lambda_{\rho\rho}^{-1} + \mathbf{a}_{\varsigma\varsigma}^{-\top}\mathbf{a}_{\rho\varsigma}^\top\Lambda_{\rho\rho}^{-1}, \quad (\text{A11b})$$

where we have used Eq. (A10). Consequently, Eq. (A1d) is greatly simplified; it reads

$$\begin{pmatrix} \mathbf{I}_\rho & \mathbf{0}_{\rho\varsigma} \\ \mathbf{a}_{\rho\varsigma}^\top\mathbf{d}_{\rho\rho} + \mathbf{a}_{\rho\varsigma}^\top\mathbf{d}_{\varsigma\rho} - \mathbf{c}_{\rho\varsigma}^\top\Lambda_{\rho\rho} & \mathbf{I}_\varsigma \end{pmatrix} = \mathbf{I}_N. \quad (\text{A12})$$

We therefore obtain

$$\mathbf{c}_{\rho\varsigma} = \Lambda_{\rho\rho}^{-1}\mathbf{d}_{\rho\rho}^\top\mathbf{a}_{\rho\varsigma} + \Lambda_{\rho\rho}^{-1}\mathbf{d}_{\varsigma\rho}^\top\mathbf{a}_{\varsigma\varsigma}. \quad (\text{A13})$$

Finally, since $\mathbf{a}_{\varsigma\varsigma}$ is invertible, both Eq. (A1e) and Eq. (A1f) take the form

$$\begin{pmatrix} \mathbf{0}_{\rho\rho} & \mathbf{0}_{\rho\varsigma} \\ \mathbf{0}_{\varsigma\rho} & \mathbf{n} - \mathbf{n}^\top \end{pmatrix} = \mathbf{0}_N, \quad (\text{A14})$$

where

$$\mathbf{n} \doteq \mathbf{a}_{\varsigma\varsigma}^\top\mathbf{d}_{\varsigma\rho}\Lambda_{\rho\rho}^{-1}\mathbf{a}_{\rho\varsigma} - \mathbf{a}_{\varsigma\varsigma}^\top\mathbf{c}_{\varsigma\varsigma}. \quad (\text{A15})$$

We therefore require $\mathbf{c}_{\varsigma\varsigma}$ to satisfy

$$\mathbf{a}_{\varsigma\varsigma}^\top\mathbf{d}_{\varsigma\rho}\Lambda_{\rho\rho}^{-1}\mathbf{a}_{\rho\varsigma} - \mathbf{a}_{\varsigma\varsigma}^\top\mathbf{c}_{\varsigma\varsigma} = (\mathbf{a}_{\varsigma\varsigma}^\top\mathbf{d}_{\varsigma\rho}\Lambda_{\rho\rho}^{-1}\mathbf{a}_{\rho\varsigma} - \mathbf{a}_{\varsigma\varsigma}^\top\mathbf{c}_{\varsigma\varsigma})^\top. \quad (\text{A16})$$

Appendix B: Derivation of equation (49)

Here, we derive Eq. (49) as the limit of $M(\mathbf{Q}, \mathbf{q}; \mathbf{S}_\varepsilon)$ at $\varepsilon \rightarrow 0$. First, we obtain, using Eq. (17),

$$M(\mathbf{Q}, \mathbf{q}; \mathbf{S}_\varepsilon) = \frac{\sigma \exp[i\tilde{G}(\mathbf{q}, \mathbf{Q})]}{(2\pi i)^{N/2} \sqrt{\det(\tilde{\mathbf{B}} + \varepsilon\tilde{\mathbf{A}})}}, \quad (\text{B1})$$

where we have defined

$$\begin{aligned} \tilde{G}(\mathbf{q}, \mathbf{Q}) &\doteq \frac{1}{2}(\mathbf{L}^\top\mathbf{Q})^\top (\tilde{\mathbf{D}} + \varepsilon\tilde{\mathbf{C}}) (\tilde{\mathbf{B}} + \varepsilon\tilde{\mathbf{A}})^{-1} \mathbf{L}^\top\mathbf{Q} \\ &\quad - (\mathbf{R}^\top\mathbf{q})^\top (\tilde{\mathbf{B}} + \varepsilon\tilde{\mathbf{A}})^{-1} \left(\mathbf{L}^\top\mathbf{Q} + \frac{1}{2}\tilde{\mathbf{A}}\mathbf{R}^\top\mathbf{q} \right) \end{aligned} \quad (\text{B2})$$

and used the unitarity of \mathbf{L} and \mathbf{R} . Next, we must approximate the matrix inverse term to leading order in ε . Let us adopt the parameterization

$$(\tilde{\mathbf{B}} + \varepsilon\tilde{\mathbf{A}})^{-1} = \begin{pmatrix} \mathbf{m}_{\rho\rho} & \mathbf{m}_{\rho\varsigma} \\ \mathbf{m}_{\varsigma\rho} & \mathbf{m}_{\varsigma\varsigma} \end{pmatrix}. \quad (\text{B3})$$

Then, since

$$\begin{pmatrix} \mathbf{m}_{\rho\rho}(\Lambda_{\rho\rho} + \varepsilon\mathbf{a}_{\rho\rho}) & \varepsilon(\mathbf{m}_{\rho\rho}\mathbf{a}_{\rho\varsigma} + \mathbf{m}_{\rho\varsigma}\mathbf{a}_{\varsigma\varsigma}) \\ \mathbf{m}_{\varsigma\rho}(\Lambda_{\rho\rho} + \varepsilon\mathbf{a}_{\rho\rho}) & \varepsilon(\mathbf{m}_{\varsigma\rho}\mathbf{a}_{\rho\varsigma} + \mathbf{m}_{\varsigma\varsigma}\mathbf{a}_{\varsigma\varsigma}) \end{pmatrix} = \mathbf{I}_N, \quad (\text{B4})$$

we require

$$\mathbf{m}_{\varsigma\rho}(\Lambda_{\rho\rho} + \varepsilon\mathbf{a}_{\rho\rho}) = \mathbf{0}_{\varsigma\rho}, \quad (\text{B5a})$$

$$\varepsilon(\mathbf{m}_{\rho\rho}\mathbf{a}_{\rho\varsigma} + \mathbf{m}_{\rho\varsigma}\mathbf{a}_{\varsigma\varsigma}) = \mathbf{0}_{\rho\varsigma}, \quad (\text{B5b})$$

$$\varepsilon(\mathbf{m}_{\varsigma\rho}\mathbf{a}_{\rho\varsigma} + \mathbf{m}_{\varsigma\varsigma}\mathbf{a}_{\varsigma\varsigma}) = \mathbf{I}_\varsigma, \quad (\text{B5c})$$

$$\mathbf{m}_{\rho\rho}(\Lambda_{\rho\rho} + \varepsilon\mathbf{a}_{\rho\rho}) = \mathbf{I}_\rho. \quad (\text{B5d})$$

Solving Eqs. (B5) in sequence yields

$$\mathbf{m}_{\varsigma\rho} = \mathbf{0}_{\varsigma\rho}, \quad \mathbf{m}_{\rho\varsigma} = -\mathbf{m}_{\rho\rho}\mathbf{a}_{\rho\varsigma}\mathbf{a}_{\varsigma\varsigma}^{-1}, \quad (\text{B6a})$$

$$\mathbf{m}_{\varsigma\varsigma} = \varepsilon^{-1}\mathbf{a}_{\varsigma\varsigma}^{-1}, \quad \mathbf{m}_{\rho\rho} = (\Lambda_{\rho\rho} + \varepsilon\mathbf{a}_{\rho\rho})^{-1} \approx \Lambda_{\rho\rho}^{-1}, \quad (\text{B6b})$$

where we have used the fact that $\mathbf{a}_{\varsigma\varsigma}$ is invertible. Hence, we obtain the following leading-order approximations:

$$\begin{aligned} &(\tilde{\mathbf{D}} + \varepsilon\tilde{\mathbf{C}}) (\tilde{\mathbf{B}} + \varepsilon\tilde{\mathbf{A}})^{-1} \\ &\approx \begin{pmatrix} \mathbf{d}_{\rho\rho}\Lambda_{\rho\rho}^{-1} & \Lambda_{\rho\rho}^{-1}\mathbf{d}_{\rho\varsigma}^\top \\ \mathbf{d}_{\varsigma\rho}\Lambda_{\rho\rho}^{-1} & \varepsilon^{-1}\mathbf{a}_{\varsigma\varsigma}^{-\top}\mathbf{a}_{\varsigma\varsigma}^{-1} + \mathbf{c}_{\varsigma\varsigma}\mathbf{a}_{\varsigma\varsigma}^{-1} - \mathbf{d}_{\varsigma\rho}\Lambda_{\rho\rho}^{-1}\mathbf{a}_{\rho\varsigma}\mathbf{a}_{\varsigma\varsigma}^{-1} \end{pmatrix}, \end{aligned} \quad (\text{B7})$$

$$(\tilde{\mathbf{B}} + \varepsilon\tilde{\mathbf{A}})^{-1} \tilde{\mathbf{A}} \approx \begin{pmatrix} \Lambda_{\rho\rho}^{-1}\mathbf{a}_{\rho\rho} & \mathbf{0}_{\rho\varsigma} \\ \mathbf{0}_{\varsigma\rho} & \varepsilon^{-1}\mathbf{I}_\varsigma \end{pmatrix}. \quad (\text{B8})$$

Upon introducing the vector decompositions

$$\mathbf{R}^\top\mathbf{x} = \begin{pmatrix} \mathbf{x}_\rho \\ \mathbf{x}_\varsigma \end{pmatrix}, \quad \mathbf{L}^\top\mathbf{y} = \begin{pmatrix} \mathbf{y}_\rho \\ \mathbf{y}_\varsigma \end{pmatrix} \quad (\text{B9})$$

(where all subvectors \mathbf{v}_n are size $n \times 1$), we obtain

$$\begin{aligned} \tilde{G}(\mathbf{q}, \mathbf{Q}) &\approx \frac{1}{2\varepsilon} |\mathbf{q}_\varsigma - \mathbf{a}_{\varsigma\varsigma}^{-1}\mathbf{Q}_\varsigma|^2 + \frac{1}{2}\mathbf{q}_\rho^\top\Lambda_{\rho\rho}^{-1}\mathbf{a}_{\rho\rho}\mathbf{q}_\rho \\ &\quad - \mathbf{q}_\rho^\top\mathbf{M}_1\mathbf{L}^\top\mathbf{Q} + \frac{1}{2}\mathbf{Q}^\top\mathbf{L}\mathbf{M}_2\mathbf{L}^\top\mathbf{Q}, \end{aligned} \quad (\text{B10})$$

where the matrices \mathbf{M}_1 and \mathbf{M}_2 are defined in Eqs. (51).

Appendix C: Metaplectic transforms in the mixed basis of configuration and coherent states

Here, we derive Eq. (72) using Gaussian coherent states. To help with the presentation, in this section, we employ the bra-ket notation of quantum mechanics [50].

The Gaussian coherent states, denoted $|\mathbf{Z}_0\rangle$, are defined by their \mathbf{Q} -space representations

$$\langle \mathbf{Q} | \mathbf{Z}_0 \rangle = \frac{\exp \left[-\frac{|\mathbf{Q} - \mathbf{Q}_0|^2}{2} + i \mathbf{K}_0^\top \left(\mathbf{Q} - \frac{\mathbf{Q}_0}{2} \right) \right]}{\pi^{N/4}}, \quad (\text{C1})$$

where $|\mathbf{Q}\rangle$ are the eigenstates of the \mathbf{Q} -space position operator $\hat{\mathbf{Q}}$, normalized as $\langle \mathbf{Q} | \mathbf{Q}' \rangle = \delta(\mathbf{Q} - \mathbf{Q}')$. The parameters \mathbf{Q}_0 and \mathbf{K}_0 define the center of $|\mathbf{Z}_0\rangle$ in phase space, that is,

$$\langle \mathbf{Z}_0 | \hat{\mathbf{Q}} | \mathbf{Z}_0 \rangle = \mathbf{Q}_0, \quad \langle \mathbf{Z}_0 | \hat{\mathbf{P}} | \mathbf{Z}_0 \rangle = \mathbf{K}_0, \quad (\text{C2})$$

where $\hat{\mathbf{P}}$ is the \mathbf{Q} -space momentum operator. The states $|\mathbf{Z}_0\rangle$ also satisfy a completeness relation of the form

$$\hat{1} = \int \frac{d\mathbf{Q}_0 d\mathbf{K}_0}{(2\pi)^N} |\mathbf{Z}_0\rangle \langle \mathbf{Z}_0|, \quad (\text{C3})$$

where $\hat{1}$ denotes the identity operator.

Let us denote $\psi_t(\mathbf{q})$ by $\langle \mathbf{q} | \psi_t \rangle$ and $\Psi_t(\mathbf{Q})$ by $\langle \mathbf{Q} | \psi_t \rangle$. Then, the inverse MT of Eq. (34) can be written as

$$\psi_t(\mathbf{q}) = \int d\mathbf{Q} \langle \mathbf{q} | \mathbf{Q} \rangle \langle \mathbf{Q} | \psi_t \rangle = \int d\mathbf{Q} \langle \mathbf{q} | \mathbf{Q} \rangle \Psi_t(\mathbf{Q}), \quad (\text{C4})$$

where we have used the completeness of $|\mathbf{Q}\rangle$, that is,

$$\hat{1} = \int d\mathbf{Q} |\mathbf{Q}\rangle \langle \mathbf{Q}|. \quad (\text{C5})$$

The matrix element $\langle \mathbf{q} | \mathbf{Q} \rangle$ is the inverse MT kernel. Direct computation of $\langle \mathbf{q} | \mathbf{Q} \rangle$ will yield Eq. (35), which is delta-shaped when $\det \mathbf{B}_t = 0$. However, by introducing the normalizable states $|\mathbf{Z}_0\rangle$ as

$$\langle \mathbf{q} | \mathbf{Q} \rangle = \int \frac{d\mathbf{Q}_0 d\mathbf{K}_0}{(2\pi)^N} \langle \mathbf{q} | \mathbf{Z}_0 \rangle \langle \mathbf{Z}_0 | \mathbf{Q} \rangle, \quad (\text{C6})$$

a nonsingular representation of the MT can be obtained. Indeed, as shown in Ref. [23],

$$\langle \mathbf{q} | \mathbf{Z}_0 \rangle = \frac{\sigma_t \exp \left[-\frac{1}{2} \mathbf{q}^\top (\mathbf{D}_t - i\mathbf{B}_t)^{-1} (\mathbf{A}_t + i\mathbf{C}_t) \mathbf{q} \right]}{\pi^{N/4} \sqrt{\det(\mathbf{D}_t - i\mathbf{B}_t)}} \times \exp \left[\left(\mathbf{q} - \frac{i}{2} \mathbf{B}_t^\top \boldsymbol{\zeta} \right)^\top (\mathbf{D}_t - i\mathbf{B}_t)^{-1} \boldsymbol{\zeta} - \frac{1}{2} \mathbf{Q}_0^\top \boldsymbol{\zeta} \right], \quad (\text{C7})$$

where we have introduced the complex vector $\boldsymbol{\zeta} \doteq \mathbf{Q}_0 + i\mathbf{K}_0$. Importantly, the complex matrix $\mathbf{D}_t - i\mathbf{B}_t$ is always invertible [29]. Then, upon using $\langle \mathbf{Z}_0 | \mathbf{Q} \rangle = (\langle \mathbf{Q} | \mathbf{Z}_0 \rangle)^*$, one computes

$$\langle \mathbf{q} | \mathbf{Z}_0 \rangle \langle \mathbf{Z}_0 | \mathbf{Q} \rangle = \frac{\sigma_t \exp \left[-\frac{1}{2} \mathbf{q}^\top (\mathbf{D}_t - i\mathbf{B}_t)^{-1} (\mathbf{A}_t + i\mathbf{C}_t) \mathbf{q} \right]}{\pi^{N/2} \sqrt{\det(\mathbf{D}_t - i\mathbf{B}_t)}} \times \exp \left[\left(\mathbf{q} - \frac{i}{2} \mathbf{B}_t^\top \boldsymbol{\zeta} \right)^\top (\mathbf{D}_t - i\mathbf{B}_t)^{-1} \boldsymbol{\zeta} - |\mathbf{Q}_0|^2 - \frac{|\mathbf{Q}|^2}{2} + \mathbf{Q}^\top \boldsymbol{\zeta}^* \right]. \quad (\text{C8})$$

Finally, we integrate over \mathbf{Q}_0 in Eq. (C6) to obtain Eq. (72). Note that \mathbf{K}_0 cannot be integrated over without inverting \mathbf{B}_t .

-
- [1] Y. A. Kravtsov and Y. I. Orlov, *Geometrical Optics of Inhomogeneous Media* (Berlin: Springer, 1990).
- [2] E. R. Tracy, A. J. Brizard, A. S. Richardson, and A. N. Kaufman, *Ray Tracing and Beyond: Phase Space Methods in Plasma Wave Theory* (Cambridge: Cambridge University Press, 2014).
- [3] Y. A. Kravtsov and Y. I. Orlov, *Caustics, Catastrophes and Wave Fields* (Berlin: Springer, 1993).
- [4] M. V. Berry, *Adv. Phys.* **25**, 1 (1976).
- [5] M. V. Berry and C. Upstill, *Prog. Opt.* **18**, 257 (1980).
- [6] C. A. Hobbs, J. N. L. Connor, and N. P. Kirk, *J. Comput. Appl. Math.* **207**, 192 (2007).
- [7] R. Borghi, *Prog. Opt.* **61**, 1 (2016).
- [8] A. Zannotti, F. Diebel, M. Boguslawski, and C. Denz, *New J. Phys.* **19**, 053004 (2017).
- [9] E. Espindola-Ramos, G. Silva-Ortigoza, C. T. Sosa-Sanchez, I. Julian-Macias, O. d. Cabrera-Rosas, P. Ortega-Vidals, A. Gonzalez-Juarez, R. Silva-Ortigoza, M. P. Velazquez-Quesada, and G. F. Torres del Castillo, *J. Opt. Soc. Am. A* **36**, 1820 (2019).
- [10] J. C. Wright, P. T. Bonoli, A. E. Schmidt, C. K. Phillips, E. J. Valeo, R. W. Harvey, and M. A. Brambilla, *Phys. Plasmas* **16**, 072502 (2009).
- [11] S. Shiraiwa, O. Meneghini, R. Parker, P. Bonoli, M. Garrett, M. C. Kaufman, J. C. Wright, and S. Wukitch, *Phys. Plasmas* **17**, 056119 (2010).
- [12] J. F. Myatt, R. K. Follett, J. G. Shaw, D. H. Edgell, D. H. Froula, I. V. Igumenshchev, and V. N. Goncharov, *Phys. Plasmas* **24**, 056308 (2017).
- [13] V. P. Maslov and M. V. Fedoriuk, *Semiclassical Approximation in Quantum Mechanics* (Dordrecht, Netherlands: Reidel, 1981).
- [14] N. A. Lopez and I. Y. Dodin, *J. Opt. Soc. Am. A* **36**, 1846 (2019).
- [15] N. A. Lopez and I. Y. Dodin, *New J. Phys.* **22**, 083078 (2020).
- [16] M. Garcia-Bulle, W. Lassner, and K. B. Wolf, *J. Math. Phys.* **27**, 29 (1986).
- [17] H. Bacry and M. Cadilhac, *Phys. Rev. A* **23**, 2533 (1981).
- [18] E. C. G. Sudarshan, R. Simon, and N. Mukunda, *Phys. Rev. A* **28**, 2921 (1983).
- [19] N. Mukunda, R. Simon, and E. C. G. Sudarshan, *Phys.*

- Rev. A **28**, 2933 (1983).
- [20] V. I. Arnold, *Russ. Math. Surv.* **30**, 1 (1975).
- [21] I. Y. Dodin, D. E. Ruiz, K. Yanagihara, Y. Zhou, and S. Kubo, *Phys. Plasmas* **26**, 072110 (2019).
- [22] I. Y. Dodin, A. I. Zhmoginov, and D. E. Ruiz, *Phys. Lett. A* **381**, 1411 (2017).
- [23] R. G. Littlejohn, *Phys. Rep.* **138**, 193 (1986).
- [24] A. W. Lohmann, *J. Opt. Soc. Am. A* **10**, 2181 (1993).
- [25] E. J. Heller, *J. Chem. Phys.* **66**, 5777 (1977).
- [26] C. Chester, B. Friedman, and F. Ursell, *Proc. Cambridge Philos. Soc.* **53**, 599 (1957).
- [27] N. Bleistein and R. A. Handelsman, *Asymptotic expansions of integrals* (New York: Dover, 1986).
- [28] M. O. Scully and M. S. Zubairy, *Quantum Optics* (Cambridge: Cambridge University Press, 2012).
- [29] R. G. Littlejohn and J. M. Robbins, *Phys. Rev. A* **36**, 2953 (1987).
- [30] F. W. J. Olver, D. W. Lozier, R. F. Boisvert, and C. W. Clark, *NIST Handbook of Mathematical Functions* (Cambridge: Cambridge University Press, 2010).
- [31] H. Kogelnik and T. Li, *Appl. Opt.* **5**, 1550 (1966).
- [32] R. B. Paris, *Proc. R. Soc. A* **432**, 391 (1991).
- [33] F. J. Wright, *J. Phys. A: Math. Gen.* **13**, 2913 (1980).
- [34] K. Y. Bliokh and Y. P. Bliokh, *Phys. Rev. E* **70**, 026605 (2004).
- [35] K. Y. Bliokh and Y. P. Bliokh, *Phys. Lett. A* **333**, 181 (2004).
- [36] D. E. Ruiz and I. Y. Dodin, *Phys. Plasmas* **24**, 055704 (2017).
- [37] D. E. Ruiz and I. Y. Dodin, *Phys. Rev. A* **92**, 043805 (2015).
- [38] D. E. Ruiz and I. Y. Dodin, *Phys. Lett. A* **379**, 2337 (2015).
- [39] D. E. Ruiz, C. L. Ellison, and I. Y. Dodin, *Phys. Rev. A* **92**, 062124 (2015).
- [40] D. E. Ruiz, *A geometric theory of waves and its applications to plasma physics*, Ph.D. thesis, Princeton University (2017).
- [41] M. A. Oancea, J. Joudioux, I. Y. Dodin, D. E. Ruiz, C. F. Paganini, and L. Andersson, *Phys. Rev. D* **102**, 024075 (2020).
- [42] K. Y. Bliokh, F. J. Rodriguez-Fortuno, F. Nori, and A. V. Zayats, *Nat. Photon.* **9**, 796 (2015).
- [43] K. Yanagihara, I. Y. Dodin, and S. Kubo, *Phys. Plasmas* **26**, 072111 (2019).
- [44] K. Yanagihara, I. Y. Dodin, and S. Kubo, *Phys. Plasmas* **26**, 072112 (2019).
- [45] I. Y. Dodin, D. E. Ruiz, and S. Kubo, *Phys. Plasmas* **24**, 122116 (2017).
- [46] Y. A. Kravtsov, O. N. Naida, and A. A. Fuki, *Phys.-Usp.* **39**, 129 (1996).
- [47] Y. A. Kravtsov, B. Bieg, and K. Y. Bliokh, *J. Opt. Soc. Am. A* **24**, 3388 (2007).
- [48] K. Y. Bliokh, D. Y. Frolov, and Y. A. Kravtsov, *Phys. Rev. A* **75**, 053821 (2007).
- [49] R. K. Luneburg, *Mathematical Theory of Optics* (Berkeley: U. California Press, 1964).
- [50] D. Stoler, *J. Opt. Soc. Am.* **71**, 334 (1981).